Archives of Gerontology and Geriatrics 54 (2012) e102–e108

Contents lists available at SciVerse ScienceDirect

Archives of Gerontology and Geriatrics

journal homepage: www.elsevier.com/locate/archger

Maladaptive turning and gaze behavior induces impaired stepping on multiple footfall targets during gait in older individuals who are at high risk of falling

Minoru Yamada [a,*], Takahiro Higuchi [b], Shuhei Mori [a], Kazuki Uemura [c], Koutatsu Nagai [a], Tomoki Aoyama [a], Noriaki Ichihashi [a]

[a] Department of Human Health Sciences, Kyoto University Graduate School of Medicine, 53 Kawahara-cho, Shogoin, Sakyo-ku, Kyoto 606-8507, Japan
[b] Department of Health Promotion Science, Graduate School of Human Health Science, Tokyo Metropolitan University, 1-1 Minami-Ohsawa, Hachioji, Tokyo 192-0397, Japan
[c] Department of Physical Therapy, Graduate School of Medicine, Nagoya University, 1-1-20 Daikouminami, Higashi-ku, Nagoya 461-8673, Japan

ARTICLE INFO

Article history:
Received 18 June 2011
Received in revised form 18 August 2011
Accepted 20 August 2011
Available online 9 September 2011

Keywords:
Gaze behavior
Falls
Older
MTST

ABSTRACT

It was recently reported that the measurement of stepping accuracy while performing a new walking test, a multi-target stepping task (MTST), could contribute to identifying older individuals at high risk (HR) of falling. The present study was designed to identify factors leading HR older individuals to an impaired stepping performance in terms of frequency of maladaptive turning behavior (spin turn) and spatio-temporal patterns of fixations. Eleven HR (80.8 ± 3.6 years), 26 low-risk (LR) (77.1 ± 7.7 years) older individuals, and 20 younger individuals performed the MTST. For the MTST, stepping accuracy was measured with two types of failure (stepping target and avoiding distracters). The frequency of a spin turn (i.e., a crossover step) was compared among the groups. The location and duration of each fixation were also compared. The HR older and younger participants showed a higher rate of spin turns. Whereas the younger participants fixated approximately three steps ahead, the older participants directed their fixation closer toward the imminent footfall target, demonstrating their difficulty to use the visual information regarding the target in a feedforward manner. Such patterns of fixations were significantly associated with the frequency of stepping and avoidance failures. The higher rate of stepping and avoidance failures in the MTST were attributed to maladaptive turning behavior, which is potentially destabilizing, and the tendency to fixate on/around an imminent footfall target, which prevented older individuals from considering the locations of future footfall targets.

1. Introduction

Older individuals who are at high risk for a fall generally exhibit increased gait variability (Verghese et al., 2009; Brach et al., 2010), a decline in visuomotor control of foot movement (Chapman and Hollands, 2006a,b, 2007), and cognitive impairment, particularly in executive functions (Alexander et al., 2005; Persad et al., 2008; Herman et al., 2010). As a result, when instructed to step precisely on a footfall target on the ground, they show more impaired performance than older individuals who are at low risk for a fall (Chapman and Hollands, 2006b, 2007). Measurement of stepping accuracy during gait is therefore useful as a clinical tool to distinguish HR older individuals from LR older individuals.

Recently, we developed a new clinical test, a multi-target stepping task, to measure the stepping accuracy in a simplified manner (Yamada et al., 2011). In the MTST, participants were instructed to step on an assigned square (the footfall target) continuously along the 15 lines while avoiding the other squares (distracters). The results demonstrated that 64.5% of HR older participants failed to step precisely on the target at least once (referred to as a stepping failure). The HR older participants also showed a significantly higher rate of failure to avoid stepping on distracters (avoidance failure) than LR older participants. A logistic regression analysis showed a significantly high odds ratio for the stepping failure (19.365), although the very large range of 95% CI (3.28–113.95) indicated that the results need to be interpreted cautiously. These findings led us to the tentative conclusion that measuring the stepping accuracy while performing the MTST is potentially an important factor in the identification of HR older individuals.

Understanding factors contributing to enhance a predictive power of the MTST to identify HR older individuals is necessary for its clinical use and a development of an intervention technique to improve stepping accuracy while performing the MTST. For this purpose, the present study was designed to measure two behaviors while performing the MTST: turning and gaze behavior.

Inaccurate stepping performance may well result from maladaptive strategies for stepping in a different direction, i.e.,

* Corresponding author. Tel.: +81 75 751 3964; fax: +81 75 751 3909.
E-mail address: yamada@hs.med.kyoto-u.ac.jp (M. Yamada).

0167-4943/$ – see front matter © 2011 Elsevier Ireland Ltd. All rights reserved.
doi:10.1016/j.archger.2011.08.012

turning behavior. The placement of multiple targets in the MTST could lead participants to turn quickly in a different direction. HR older individuals generally show difficulty in maintaining a stabilized posture after stepping in a different direction (Dite and Temple, 2002; Tseng et al., 2009). Two main strategies for turning exist: step and spin turns. Whereas a step turn involves a change in the direction opposite to the stance limb, the spin turn is taking a crossover step, i.e., changing in the direction toward the same side of the stance limb. A spin turn is potentially destabilizing because, if appropriate pro-active action is not taken, the center of mass (COM) of the body will be outside of the base of support (BOS) (Moraes et al., 2004; Taylor et al., 2005). We hypothesized that impaired stepping performance while performing the MTST in HR older individuals was accompanied by more frequent spin turns.

Spin turns could occur more frequently when participants concentrated on stepping accurately on an imminent footfall target and did not consider the locations of future footfall targets. Measuring gaze behavior while performing the MTST was an effective approach to address this issue. By measuring how far ahead the fixation was located, we examined whether age-related differences existed in the visual scanning of footfall targets while performing the MTST.

The hypothesis regarding the location of fixation was that fixation in older individuals should be directed closer toward an imminent footfall target. The spatial demand of stepping in the MTST is relatively moderate, considering the criteria that even a step on the edge of the target was regarded as successful. Under such moderate conditions, younger individuals generally fixate a few steps ahead to step on multiple footfall targets (Patla and Vickers, 2003). This means that visual information regarding the location of an imminent footfall target is used in a feedforward manner, i.e., based on "stored" visuospatial information (Zettel et al., 2008), rather than in an on-line, feedback manner. In contrast, older individuals have difficulty using vision in a feedforward manner (Chapman and Hollands, 2006a). It was therefore hypothesized that fixation in older individuals should be directed closer toward an imminent footfall target.

To further understand the characteristics of gaze behavior in HR older individuals, we examined the duration of each fixation, particularly toward a target. Chapman and colleagues demonstrated that HR older individuals looked at targets longer when they walked while stepping on multiple footfall targets with relatively strict spatial demand (Chapman and Hollands, 2006b, 2007). With these findings, they proposed that they would require more time to process visual information regarding targets and/or program appropriate motor responses. We investigated whether a similar tendency would occur while they performed the MTST in spite of its moderate spatial demand.

Our primary analyses were to compare stepping performances, turning and gaze behaviors among the HR older, LR older, and the younger control groups. In addition, it was important to address which of several measurements were significantly associated with stepping avoidance failures. To do so, secondary analyses were conducted. Older participants were divided into two groups according to whether they had experienced stepping and avoidance failures (i.e., regardless of whether they were in the HR or older LR group). Each measurement regarding gaze behavior and other clinical measurements were compared statistically between the two groups. Furthermore, to determine whether the maladaptive spin turn occurred as a result of the participants' fixation being directed closer to the target, we conducted another statistical analysis in which the older participants were divided into two groups according to their experience of the spin turn. Comparisons of the gaze behavior were made between the two groups.

2. Methods

2.1. Participants

A total of 37 community-dwelling older individuals (mean age, 78.1 ± 6.8 years) participated. The exclusion criteria ensured that none of the participants had any indications of the following symptoms: (a) serious visual impairment (cataract, glaucoma, or color blindness), (b) inability to ambulate independently (those requiring the assistance of a walker were excluded), (c) score of less than 7 on the Rapid Dementia Screening Test (Kalbe et al., 2003), (d) symptomatic cardiovascular disease, (e) neurological and orthopedic disorders, (f) peripheral neuropathy of the lower extremities, or (g) severe arthritis. None of them had performed the MTST before. Twenty younger individuals (mean age, 21.1 ± 1.4 years) also took part in this experiment as control participants. Written informed consent was obtained from each subject in accordance with the guidelines approved by the Kyoto University Graduate School of Medicine and the Declaration of Human Rights, Helsinki, 1975.

Following an earlier study (Yamada et al., 2011), a participant who met the following two criteria was classified as an HR older individual: (a) a self-report of the occurrence of at least one fall within the past year and (b) a time requirement greater than 13.5 s for performing a Timed Up and Go test (TUG) (Shumway-Cook et al., 2000). A fall was defined as any event that led to an unplanned, unexpected contact with a supporting surface during walking. Our definition that the experience of falls was restricted to those during walking (i.e., falls during standing or transferring were not included) was suitable for the present study, considering that the MTST was developed to differentiate older HR individuals from LR ones in terms of stepping accuracy during walking. We ensured that none of the participants had any fall experience during standing or transferring.

As a result, 11 HR and 26 LR elderly individuals participated (see Table 1 for participant details). A one-way ANOVA conducted for each data of age, height, weight, the score of the Rapid Dementia Screening Test, and the visual acuity score (binocular acuity scored on the basis of a Landolt C) showed no significant differences between the HR and LR groups (Table 1). A Chi-square analysis conducted for the data of gender distribution also showed no significant differences between the HR and LR groups (Table 1).

2.2. Setup and protocols for data collection of the MTST

The MTST was performed on a black elastic mat (10 m long and 1 m wide). There were 45 pieces of a 10 cm × 10 cm square on the mat (see Fig. 1a). These squares were arranged into three rows (15 cm between each row) and 15 lines (61 cm between each line). Each square was marked with red, blue, or yellow tape. Each line had one of the three colored squares in a randomized order. One square (blue or yellow) was regarded as a footfall target, while the others were distracters.

Gaze behavior was measured using a head-mounted eye tracker (EMR-9, Nac Image Technologies, Japan). The eye tracker we used was a binocular corneal reflection system that measures the eye line of gaze with respect to a hat. The participant's gaze was indicated by a circle mark on a video-based image of the visual field as recorded by a scene camera mounted on the hat at a temporal resolution of 30 Hz (see Fig. 1b). Three-dimensional accelerometers (WAA-006, ATR-Promotions, Japan) were attached to each heel to measure the timing of participants' heel contact for each stepping.

The participants wore flat-soled footwear and walked on the mat at a self-selected pace while stepping on the target square placed on each line without stepping on the distracters. The participants performed two main trials. For each trial, a different color square was assigned as a footfall target. Detailed information

Table 1
Group comparisons of the characteristics of participants, MTST performance, gaze behavior, and other clinical tests.

	HR older ($n=11$)		LR older ($n=26$)		Younger ($n=20$)		ANOVA	
	Mean	SD	Mean	SD	Mean	SD	p value	
Participant details								
Age	80.8	3.6	77.1	7.7	21.1	1.4	<0.001*	b,c
Height, cm	155.1	8.8	153.8	10.2	164.4	9.7	<0.001*	b,c
Weight, kg	48.8	5.8	55.5	10.1	56.3	9.0	<0.001*	b
Gender (male = 0, female = 1), %	63.6		61.5		50.0			
Rapid Dementia Screening Test, point	8.91	1.13	9.27	1.60	12.00	0.00	<0.001*	b,c
Vision acuity score, decimal	0.75	0.39	0.77	0.30	0.73	0.33	0.885	
MTST performance								
Stepping failure (yes = 1, no = 0), %	72.7		7.6		0.0			a,b
Number of stepping failure, times	0.7	0.5	0.1	0.3	0.0	0.0	<0.001*	a,b
Avoidance failure (yes = 1, no = 0), %	100.0		15.3		0.0			a,b
Number of avoidance failure, times	3.7	2.9	0.5	1.6	0.0	0.0	<0.001*	a,b
Performance time, s	36.2	4.0	29.8	8.9	18.7	6.2	<0.001*	b,c
Stepping interval time, s	2.8	0.4	2.5	1.4	1.2	0.4	<0.001*	b,c
Spin (yes = 1, no = 0), %	63.6		15.3		50.0			a,c
Gaze toward target								
Gaze duration, s	0.85	0.38	0.78	0.63	0.62	0.24	0.402	
Gaze initiation, s (before stepping)	1.36	0.26	1.94	1.09	3.54	1.56	<0.001*	b,c
Gaze termination, s (before stepping)	0.52	0.42	1.17	0.97	2.91	1.60	<0.001*	a,b,c
Initiation/interval	0.50	0.09	0.89	0.53	2.94	1.21	<0.001*	a,b,c
Termination/interval	0.19	0.16	0.61	0.56	2.41	1.27	<0.001*	a,b,c
Other clinical tests								
10 m walking time, s	16.1	2.7	11.5	3.7			t-Test	
Timed Up and Go, s	19.8	4.3	13.1	4.4			0.001*	
One leg stand, s	1.2	1.5	9.3	12.7			<0.001*	
Functional reach, cm	18.3	3.9	24.1	4.7			0.005*	
5 chair stand, s	19.7	11.2	13.3	3.5			0.006*	
							0.020	

ANOVA: Bonferroni correction $p=0.016$ (0.05/3).
Post hoc test: $p<0.016$.
[a] Post hoc test: HR vs LR.
[b] Post hoc test: HR vs young.
[c] Post hoc test: LR vs young.

about the protocol of the MTST has been given in an earlier study (Yamada et al., 2011).

2.3. Data analyses of the MTST

All dependent measures were obtained only from the first main trial (Yamada et al., 2011). This was because, as other clinical standard tests used for identifying HR older individuals, the MTST had been developed so that participants could complete the task in a short time. The earlier study demonstrated that analyzing stepping performance in a single trial was effective to identify HR older individuals (Yamada et al., 2011). The stepping performance obtained from the second main trial was used only to calculate test–retest reliability.

The main dependent measures were two types of failure indicating less accurate stepping performance: a stepping failure

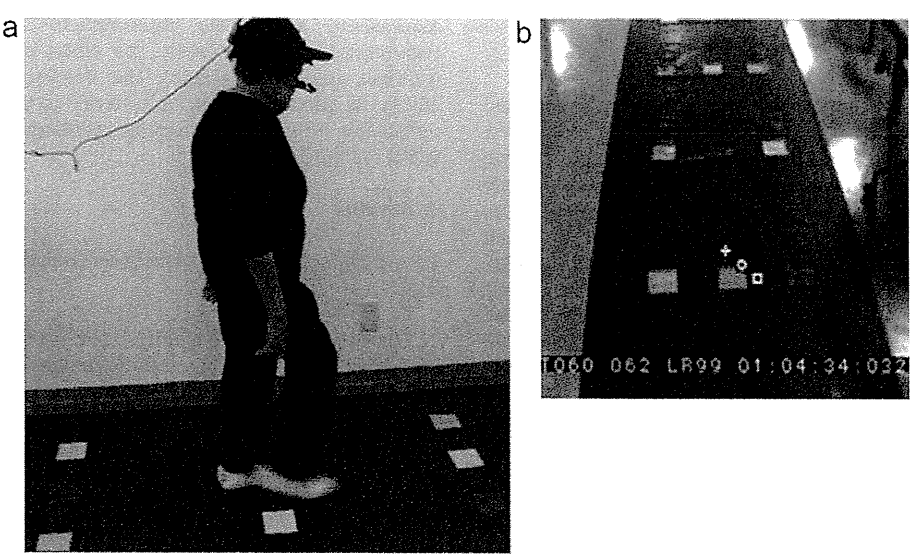

Fig. 1. (a) An older participant performing the MTST. Each square in each line was made of red, blue, or yellow tape. The participant intended to walk at a self-selected pace while stepping on a target square of an assigned color while avoiding to step on other squares. (b) A video-based image of the visual field while performing the MTST. The location of fixation, indicated by a circle mark, was calculated with the information obtained from the left (a plus mark) and right (a square mark) eyes.

(i.e., failure to step on the footfall target) and an avoidance failure (i.e., failure to avoid distracters). Even a step on the edge of the target was regarded as successful. These measures were analyzed statistically from two perspectives. First, the participants who experienced each type of failure at least once were totaled for both the HR and LR groups. For each failure, the numbers, expressed as the frequency of failure occurring in the group (%), were compared statistically among the groups with a Chi-square analysis. Secondly, the number of failures for each participant was statistically compared among the groups with a one-way analysis of variance (ANOVA). To investigate the test–retest reliability for the two types of the stepping failure, Kappa coefficients (k-values) between the two trials were calculated. A k-value of 0.61–0.80 was regarded as good agreement (Naessens et al., 2010).

The time (s) taken to perform the MTST, referred to as the MTST performance time, was measured with a stopwatch. The time of the interval between each step was also measured with the accelerometers attached to each heels. The timing of each step was defined as the time when peak acceleration occurred in the vertical direction. Each MTST performance time and stepping interval was compared statistically among the groups with a one-way ANOVA. To investigate the test–retest reliability for the MTST performance time, the inter-trial correlation coefficient (ICC 1.1) between the two trials was calculated.

Regarding the frequency of the maladaptive turning behavior (spin turn), the participants who experienced crossover steps at least once in a trial were totaled for each of the three groups. The frequencies of failure occurring in the group (%) were compared statistically among the groups with a Chi-square analysis. To investigate the test–retest reliability for the frequency of the spin turn, a k-value between the two trials was calculated.

Frame-by-frame video-based analyses were performed to identify where fixations were located. Stabilization of the gaze at one location for a minimum of 100 ms (three video frames) was defined as a fixation. The locations of fixations were classified into one of four categories: target, distracter, path, or other. The durations of each fixation were quantified and statistically compared among the groups using a one-way ANOVA. To statistically test the fixation patterns, each participant's average fixation time, as a percentage of total fixations, in each fixation-location was compared among the groups using a one-way ANOVA.

2.4. Data collection and analyses of gaze behavior

For the purpose of examining how far ahead the participants' fixations were located, the time to initiate (referred to as gaze initiation) and terminate (gaze termination) gazing at a given target before stepping on it was measured. The data of the gaze initiation (termination) were calculated by subtracting the time to initiate (terminate) fixation toward the imminent footfall target from the time to step on the target, which was obtained through the three-dimensional accelerometers attached to each heel. Dividing these timing data by the duration of the stepping interval (referred to as initiation/interval and termination/interval) expressed the degree to which the participants directed their fixation toward a future target. For instance, when the value of initiation/interval was 1.0 (i.e., the duration between the initiation of fixation toward a certain target and stepping on that target was equal to the duration of the stepping interval), a participant began to fixate a next footfall target just when stepping on the imminent footfall target. A value smaller than 1.0, therefore, meant that a fixation was directed toward the imminent target, whereas a value larger than 1.0 meant that a fixation was directed toward a future footfall target. A one-way ANOVA was used to compare these measurements statistically among the groups.

2.5. Data collection and analyses of other clinical tests

Other clinical tests that have been used to identify high-risk elderly adults in many studies, i.e., the TUG (Podsiadlo and Richardson, 1991), the functional reach test (FR) (Duncan et al., 1992), the one-leg standing test (OLS) (Vellas et al., 1997), the 10 m walking test (10 m walking) (Lopopolo et al., 2006), and the 5-chair stand (5CS) test (Guralnik et al., 1994), were measured prior to performing the MTST on the first measurement day. All tests except the 5CS were used in the earlier study (Yamada et al., 2011). In the 5CS, participants were asked to stand up and sit down five times as quickly as possible. A 5CS score was defined as the average of two trials regarding the time in seconds for the completion of this task. The order in which these tests were performed was randomized. The participants performed each task for two trials. A t-test analysis was examined for each clinical test to statistically compare the scores between the HR and LR groups.

2.6. Associations among the measurements

To quantitatively describe the associations between the stepping accuracy in the MTST and other measurements, the 37 older participants were divided into two groups according to whether they experienced both stepping and avoidance failures or not. Each of all measurements regarding gaze behavior and the clinical tests was compared statistically between the two groups with a t-test. To examine whether a spin turn was likely to occur when a participant's fixations were directed closer to an imminent footfall target, the participants were also divided into two groups according to whether they experienced a spin turn. Each of all measurements regarding gaze behavior was compared statistically between the two groups with a t-test. Furthermore, whether the experience of a spin turn was associated with the scores of the clinical tests was also analyzed. A comparison with a t-test was performed between the two groups.

2.7. Adjustment of a significance level for multiple statistical comparisons

In the present study, three different analyses were undertaken with the same data set (i.e., a comparison among the HR, LR older and young groups, and two two-group comparisons for testing associations among the measurements). To avoid a risk of committing a Type 1 error, the alpha-level was adjusted for multiple comparisons using the Bonferroni correction (Feise, 2002). In particular, the alpha-level of 0.05 was corrected to reflect five different comparisons, resulting in an adjusted alpha of 0.016 (0.05/3).

3. Results

3.1. MTST performance, gaze behavior, and clinical tests (Table 1 and Fig. 2)

The HR older participants experienced significantly higher frequency of both stepping and avoidance failures than the LR older and younger participants. The average number of each failure occurring in each group was greater for the HR older participants than for the LR older and younger participants. Both the MTST performance time and the stepping interval were significantly shorter for the younger participants than the HR and LR older participants. The HR older and younger participants experienced significantly higher frequency of the spin turns than the LR participants. The investigation of the test–retest reliability indicated that the k-value was 0.724 for the stepping failure, 0.746 for the avoidance failure, and 0.877 for the spin turn. The

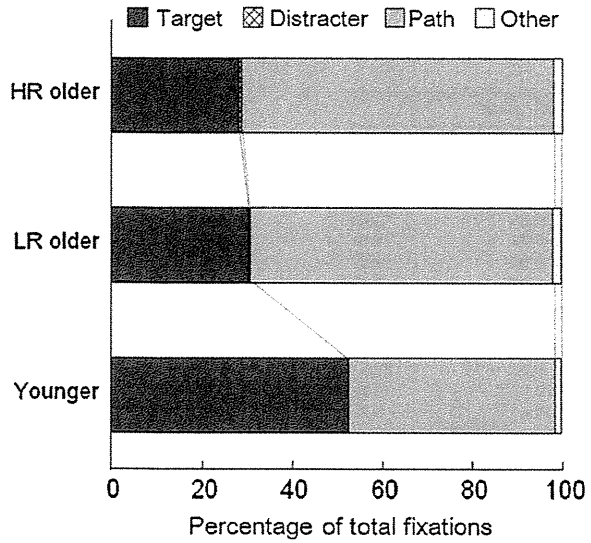

Fig. 2. Frequency of fixation directed toward each location in each group. The location-category of the distracter is not included because none of the participants fixated toward the distracters.

correlation between the first- and second-time measurements of the MTST performance time was very high (ICC = 0.969 (95%CI: 0.954–0.979)).

The group differences in the gaze duration were not statistically significant. The timing of gaze initiation was significantly earlier for the younger participants than the HR and LR older participants. The difference in this measurement was not significant between the HR and LR participants. The differences in the gaze termination, initiation/interval, and termination/interval were all significant for each pair in the three groups. The average percentages of total fixation durations (Fig. 2) showed that the fixation was directed toward the target more frequently for the younger participants than for the HR and LR older participants ($p < 0.016$). Participants rarely directed their fixation toward the distracters (0.4, 0.2, and 0% for the HR, LR, and younger groups, respectively). The younger participants directed their fixation toward the path less frequently than the HR and LR participants ($p < 0.016$).

Comparison of the performances in other clinical tests between the HR and LR participants showed that the HR older participants showed a significantly lower score than the LR older participants in all clinical tests except the 5CS.

3.2. Associations among the measurements (Tables 2 and 3)

Eight older participants experienced both stepping and avoidance failures (other two participants experienced only stepping failures, whereas seven experienced only avoidance failures). Regarding the association of stepping accuracy with gaze behavior and clinical tests (Table 2), the participants who experienced both failures initiated and terminated fixation toward an imminent target significantly later than those who did not. The mean values of initiation/interval and termination/interval were significantly greater for the participants who experienced both types of failures than for those who did not. The participants who experienced both failures showed significantly lower scores for the TUG, OLS, and FR than the participants who did not. No significant differences in all measurements on gaze behavior and on the clinical tests were identified between the participants who experienced a spin turn and those who did not (Table 3).

4. Discussion

The purpose of the present study was to examine whether maladaptive turning and gaze behavior existed while HR older individuals were performing the MTST. Before discussing this issue it is important to address that the present findings successfully replicated earlier ones (Yamada et al., 2011) regarding the fact that the HR older participants showed less stepping accuracy in the MTST. The HR older participants showed a significantly higher rate of stepping and avoidance failures than the LR older and younger participants. It is noteworthy that avoidance failure always occurred as a result of an accidental step in the way the participants were walking from target to target but not as a result of the wrong selection of a target from the three squares in the line that they intended to step on. Avoidance failure, therefore, resulted mainly from incorrect planning of the walking path from target to target and not from the wrong selection of a target from the three squares in a line due to impaired contrast sensitivity. The test–retest examination showed that these measurements were statistically reliable. These findings supported the conclusion of the earlier study (Yamada et al., 2011) that measuring the stepping accuracy while performing the MTST is potentially an important factor in the identification of HR older individuals.

Analysis of the frequency of the spin turn supported the hypothesis that impaired stepping performance in HR older individuals was accompanied with more frequent spin turns. Seven out of 11 HR older participants (63.6%) made a spin turn at least once to change their walking direction. In contrast, many of the LR older participants (22 out of 26 participants) did not select a

Table 2
Associations of the experience of stepping and avoidance failures with gaze behavior and clinical tests.

	Failure				*p* value	E/S
	Yes ($n=8$)		No ($n=29$)			
	Mean	SD	Mean	SD		
Gaze toward target						
Gaze duration, s	0.87	0.40	0.78	0.61	0.61	0.24
Gaze initiation, s (before stepping)	1.28	0.26	1.97	1.06	0.01*	2.63
Gaze termination, s (before stepping)	0.41	0.35	1.13	0.93	0.00*	2.05
Initiation/interval	0.50	0.11	0.85	0.51	0.00*	3.10
Termination/interval	0.17	0.17	0.57	0.54	0.00*	2.36
Other clinical tests						
10 m walking time, s	14.92	1.77	12.23	4.23	0.02	1.52
Timed Up and Go, s	17.67	1.75	14.41	5.75	0.01*	1.86
One leg stand, s	0.76	1.18	9.06	12.52	0.00*	7.05
Functional reach, cm	19.67	1.37	23.52	5.42	0.00*	2.82
5 chair stand, s	17.25	10.10	14.17	5.41	0.30	0.30

Bonferroni correction $p = 0.016$ (0.05/3).

Table 3
Associations of the experience of spin turns with gaze behavior and clinical tests.

	Spin turn				p value	E/S
	Yes (n=11)		No (n=26)			
	Mean	SD	Mean	SD		
Gaze toward target						
Gaze duration, s	0.80	0.36	0.79	0.64	0.959	0.020
Gaze initiation, s (before stepping)	1.49	0.47	1.89	1.09	0.127	0.850
Gaze termination, s (before stepping)	0.69	0.68	1.10	0.95	0.152	0.600
Initiation/interval	0.65	0.34	0.83	0.52	0.242	0.510
Termination/interval	0.34	0.39	0.55	0.55	0.201	0.530
Other clinical tests						
10 m walking time, s	12.6	3.3	12.8	4.4	0.917	0.040
Timed Up and Go, s	15.3	3.9	15.0	5.9	0.860	0.080
One leg stand, s	4.1	5.8	9.1	13.5	0.161	0.860
Functional reach, cm	21.3	2.9	23.5	5.9	0.193	0.750
5 chair stand, s	15.5	8.2	14.4	5.7	0.701	0.140

Bonferroni correction p=0.016 (0.05/3).

spin turn. This suggests that the LR older individuals successfully avoided the risk of destabilization while performing the MTST. The existence of such a clear difference in turning strategy between the HR and LR older participants is likely to contribute to enhancing the predictive power of the MTST to identify HR older individuals.

Interestingly, the younger participants also showed a higher rate of spin turns. A similar finding was reported in a previous study (Moraes et al., 2004), which demonstrated that their young participants preferred stepping medially (i.e., making a spin turn) rather than stepping laterally (i.e., making a step turn) to avoid a planar obstacle. The authors argued that modification of foot placement in response to an obstacle involves minimum displacement of the foot from its normal landing spot; stepping medially could be more suitable to satisfy this goal than stepping laterally. According to these previous findings, the younger participants in the present study may have not hesitated to select a spin turn because they had the ability to take pro-active action to bias the location of COM to ensure that it did not fall outside the BOS.

Analysis of gaze behavior supported another hypothesis that fixation in older individuals should be directed closer toward the imminent footfall target. The measurements of the initiation/interval and termination/interval revealed that the HR and LR older participants directed their gaze toward the imminent footfall target. Such a tendency was significantly higher for the HR older participants than the LR older ones. In contrast, the younger participants directed their gaze toward approximately 3 targets ahead. These findings clearly supported previous findings that, whereas younger individuals use visual information regarding the location of an imminent footfall target in a feedforward manner, older individuals appear to use it in an online, feedback manner (Patla and Vickers, 2003; Chapman and Hollands, 2006a).

Analyses of the association of stepping accuracy with gaze behavior demonstrated that the observed fixation patterns in the HR older participants were related to the stepping and avoidance failures (Table 2). The participants who experienced both the stepping and avoidance failures initiated and terminated fixation toward an imminent target significantly later than those who did not. From these findings, we suggest that one of the reasons for the higher rate of stepping and avoidance failures in the HR older individuals could be attributed to their tendency to fixate on/around the imminent footfall target, which prevented them from considering the locations of future footfall targets.

The HR older participants showed a higher rate of failure of stepping on the footfall targets in spite of the fact that they concentrated on fixation toward the imminent footfall target. The measurements of gaze termination showed that, on average, the HR older participants terminated fixation on the imminent footfall target approximately 0.5 s before stepping on that target. This indicated that they did not fixate on the imminent footfall target until they stepped on it; that is, the imminent footfall target was captured through peripheral vision or out of sight. The present findings suggest that the observed spatiotemporal patterns of fixation toward the imminent footfall target in the HR older participants may not have led to accurate foot control for stepping on a footfall target. Similarly, the average percentages of total fixation durations (Fig. 2) demonstrated that the participants rarely fixated toward the distracters (only 0.4% of total fixation times for the HR older, 0.2% for the LR older, and 0% for the younger participants). This suggests that the information regarding the locations of the distracters was obtained through peripheral vision (Patla and Vickers, 1997; Zietz and Hollands, 2009; Miyasike-daSilva et al., 2011). The failure to avoid the distractors may have resulted from their impaired ability to control their foot placement based on peripheral vision (Di Fabio et al., 2005).

The duration of fixation was not significantly different among the groups. This was inconsistent with previous findings demonstrating that HR individuals looked at footfall targets longer (Chapman and Hollands, 2006b, 2007). The contradictory findings between the previous and present studies may have been attributed to the difference in the spatial demand for stepping between these studies. In other words, a longer target fixation of the target would have been necessary when the spatial demand for stepping on the target was relatively strict, as in previous studies. Alternatively, given that the fixation was directed toward the path more frequently for the HR and LR older participants (Fig. 2), fixation on the place of each step, rather than on the target alone, may have been necessary while the HR older participants were performing the MTST. As a result, they may not have directed their fixation toward the target for a particularly longer time.

Theoretically, a spin turn could occur more frequently as fixation was located closer toward the imminent footfall target and, as a result, the locations of future footfall targets were not considered. However, we failed to demonstrate a significant association between the frequency of the spin turn and the pattern of fixations (Table 3). In fact, the experience of a spin turn was not significantly associated with any measurements about gaze behavior and other clinical tests. The precise mechanism for causing maladaptive turning behavior remains unclear. A future study should address this issue.

Analyses of the association of stepping accuracy with other clinical measurements demonstrated that the participants who experienced both stepping and avoidance failures showed lower scores for the TUG, OLS, and FR (Table 2). This was generally consistent with the findings in our earlier study (Yamada et al.,

2011), which demonstrated that the number of avoidance failures showed mild negative correlation with the performance of the TUG and OLS. These findings suggest that impaired stepping performance in the MTST was likely to be associated with the impairment of general balance abilities, lower extremity function, and mobility.

In conclusion, the present study demonstrated impaired stepping performance of the HR older individuals in the MTST was accompanied with their maladaptive turning and gaze behavior. One of the most important findings was that the HR older individuals fixated closer toward the imminent footfall target. This suggests that they have difficulty in using visual information regarding the location of an imminent footfall target in a feedforward manner. Such a pattern of fixations would prevent them from considering the locations of future footfall targets and, therefore, can cause a maladaptive strategy to step in a different direction. In fact, the stepping performance in HR older individuals was accompanied with more frequent spin turns. Due to the lack of a significant association of the spin turn with the patterns of fixations, future studies should identify a precise mechanism for selecting the maladaptive turning behavior.

Funding

None.

Conflict of interest statement

None.

References

Alexander, N.B., Ashton-Miller, J.A., Giordani, B., Guire, K., Schultz, A.B., 2005. Age differences in timed accurate stepping with increasing cognitive and visual demand: a walking trail making test. J. Gerontol. A: Biol. Sci. Med. Sci. 60, 1558–1562.

Brach, J.S., Perera, S., Studenski, S., Katz, M., Hall, C., Verghese, J., 2010. Meaningful change in measures of gait variability in older adults. Gait Posture 31, 175–179.

Chapman, G.J., Hollands, M.A., 2006a. Age-related differences in stepping performance during step cycle-related removal of vision. Exp. Brain Res. 174, 613–621.

Chapman, G.J., Hollands, M.A., 2006b. Evidence for a link between changes to gaze behaviour and risk of falling in older adults during adaptive locomotion. Gait Posture 24, 288–294.

Chapman, G.J., Hollands, M.A., 2007. Evidence that older adult fallers prioritise the planning of future stepping actions over the accurate execution of ongoing steps during complex locomotor tasks. Gait Posture 26, 59–67.

Di Fabio, R.P., Zampieri, C., Henke, J., Olson, K., Rickheim, D., Russell, M., 2005. Influence of elderly executive cognitive function on attention in the lower visual field during step initiation. Gerontology 51, 94–107.

Dite, W., Temple, V.A., 2002. A clinical test of stepping and change of direction to identify multiple falling older adults. Arch. Phys. Med. Rehabil. 83, 1566–1571.

Duncan, P.W., Studenski, S., Chandler, J., Prescott, B., 1992. Functional reach: predictive validity in a sample of elderly male veterans. J. Gerontol. 47, M93–M98.

Feise, R.J., 2002. Do multiple outcome measures require *p*-value adjustment? BMC Med. Res. Methodol. 2, 1–4.

Guralnik, J.M., Simonsick, E.M., Ferrucci, L., Glynn, R.J., Berkman, L.F., Blazer, D.G., Scherr, P.A., Wallace, R.B., 1994. A short physical performance battery assessing lower extremity function: association with self-reported disability and prediction of mortality and nursing home admission. J. Gerontol. 49, M85–M94.

Herman, T., Mirelman, A., Giladi, N., Schweiger, A., Hausdorff, J.M., 2010. Executive control deficits as a prodrome to falls in healthy older adults: a prospective study linking thinking, walking, and falling. J. Gerontol. A: Biol. Sci. Med. Sci. 65, 1086–1092.

Kalbe, E., Calabrese, P., Scgwalen, S., Kessler, J., 2003. The Rapid Dementia Screening Test (RDST): a new economical tool for detecting possible patients with dementia. Dement. Geriatr. Cogn. Disord. 16, 193–199.

Lopopolo, R.B., Greco, M., Sullivan, D., Craik, R.L., Mangione, K.K., 2006. Effect of therapeutic exercise on gait speed in community-dwelling elderly people: a meta-analysis. Phys. Ther. 86, 520–540.

Miyasike-daSilva, V., Allard, F., McIlroy, W.E., 2011. Where do we look when we walk on stairs? Gaze behaviour on stairs, transitions, and handrails. Exp. Brain Res. 209, 73–83.

Moraes, R., Lewis, M.A., Patla, A.E., 2004. Strategies and determinants for selection of alternate foot placement during human locomotion: influence of spatial and temporal constraints. Exp. Brain Res. 159, 1–13.

Naessens, J.M., O'Byrne, T.J., Johnson, M.G., Vansuch, M.B., McGlone, C.M., Huddleston, J.M., 2010. Measuring hospital adverse events: assessing inter-rater reliability and trigger performance of the Global Trigger Tool. Int. J. Qual. Health Care 22, 266–274.

Patla, A.E., Vickers, J.N., 1997. Where and when do we look as we approach and step over an obstacle in the travel path? Neuroreport 8, 3661–3665.

Patla, A.E., Vickers, J.N., 2003. How far ahead do we look when required to step on specific locations in the travel path during locomotion? Exp. Brain Res. 148, 133–138.

Persad, C.C., Jones, J.L., Ashton-Miller, J.A., Alexander, N.B., Giordani, B., 2008. Executive function and gait in older adults with cognitive impairment. J. Gerontol. A: Biol. Sci. Med. Sci. 63, 1350–1355.

Podsiadlo, D., Richardson, S., 1991. The Timed Up & Go: a test of basic functional mobility for frail elderly persons. J. Am. Geriatr. Soc. 39, 142–148.

Shumway-Cook, A., Brauer, S., Woollacott, M., 2000. Predicting the probability for falls in community-dwelling older adults using the Timed Up & Go Test. Phys. Ther. 80, 896–903.

Taylor, M.J., Dabnichki, P., Strike, S.C., 2005. A three-dimensional biomechanical comparison between turning strategies during the stance phase of walking. Hum. Mov. Sci. 24, 558–573.

Tseng, S.C., Stanhope, S.J., Morton, S.M., 2009. Impaired reactive stepping adjustments in older adults. J. Gerontol. A: Biol. Sci. Med. Sci. 64, 807–815.

Vellas, B.J., Wayne, S.J., Romero, L., Baumgartner, R.N., Rubenstein, L.Z., Garry, P.J., 1997. One-leg balance is an important predictor of injurious falls in older persons. J. Am. Geriatr. Soc. 45, 735–738.

Verghese, J., Holtzer, R., Lipton, R.B., Wang, C., 2009. Quantitative gait markers and incident fall risk in older adults. J. Gerontol. A: Biol. Sci. Med. Sci. 64, 896–901.

Yamada, M., Higuchi, T., Tanaka, B., Nagai, K., Uemura, K., Aoyama, T., Ichihashi, N., 2011. Measurements of stepping accuracy in a multi-target stepping task as a potential indicator of fall risk in elderly individuals. J. Gerontol. A: Biol. Sci. Med. Sci. 66, 994–1000.

Zettel, J.L., McIlroy, W.E., Maki, B.E., 2008. Gaze behavior of older adults during rapid balance-recovery reactions. J. Gerontol. A: Biol. Sci. Med. Sci. 63, 885–891.

Zietz, D., Hollands, M., 2009. Gaze behavior of young and older adults during stair walking. J. Mot. Behav. 41, 357–365.

Rheumatol Int
DOI 10.1007/s00296-011-2283-2

ORIGINAL ARTICLE

Objective assessment of abnormal gait in patients with rheumatoid arthritis using a smartphone

Minoru Yamada · Tomoki Aoyama · Shuhei Mori · Shu Nishiguchi · Kazuya Okamoto · Tatsuaki Ito · Shinyo Muto · Tatsuya Ishihara · Hiroyuki Yoshitomi · Hiromu Ito

Received: 2 August 2011 / Accepted: 10 December 2011

Abstract A disturbance in gait pattern is a serious problem in patients with rheumatoid arthritis (RA). The aim of the present study was to examine the utility of the smartphone gait analysis application in patients with RA. The smartphone gait analysis application was used to assess 39 patients with RA (age 65.9 ± 10.0 years, disease duration 11.9 ± 9.4 years) and age-matched control individuals (mean age, 69.1 ± 5.8 years). For all RA patients, the following data were obtained: disease activity score (DAS) 28, modified health assessment questionnaire (mHAQ), and assessment of walking ability. Patients walked 20 m at their preferred speed, and trunk acceleration was measured using a Smartphone. After signal processing, we calculated the following gait parameters for each measurement terminal: peak frequency (PF), autocorrelation peak (AC), and coefficient of variance (CV) of the acceleration peak intervals. The gait parameters of RA and control groups were compared to examine the comparability of the 2 groups. Criterion-related validity was determined by evaluating the correlation between gait parameters and clinical parameters using Spearman's correlation coefficient. The RA group showed significantly lower scores for the walking speed, AC, and CV than the control group. There were no significant differences in PF. PF (gait cycle) was mildly associated with gait speed ($P < 0.05$). AC (gait balance) was moderately associated with the DAS, mHAQ, gait ability, and gait speed ($P < 0.05$). CV (gait variability) was moderately associated with the DAS, gait ability, and gait speed ($P < 0.05$). This is the first study to examine the use of a smartphone device for gait pattern measurement. The results suggest that some gait parameters recorded using the smartphone represent an acceptable assessment tool for gait in patients with RA.

Keywords Smartphone · Gait analysis · Validity · Rheumatoid arthritis

M. Yamada (✉) · T. Aoyama · S. Mori · S. Nishiguchi
Human Health Sciences, Graduate School of Medicine, Kyoto University, 53 Kawahara-cho, Shogoin, Sakyo-ku, Kyoto 606-8507, Japan
e-mail: yamada@hs.med.kyoto-u.ac.jp

K. Okamoto
Department of Medical Informatics, Kyoto University Hospital, Kyoto, Japan

T. Ito · S. Muto
NTT Cyber Solutions Laboratories, Yokosuka, Japan

T. Ishihara
Nippon Telegraph and Telephone East Corporation, Sapporo, Japan

H. Yoshitomi
Department of Orthopaedic Surgery, Graduate School of Medicine, Kyoto University, Kyoto, Japan

H. Ito
Department for the Control of Rheumatic Diseases, Graduate School of Medicine, Kyoto University, Kyoto, Japan

Introduction

Rheumatoid arthritis (RA) affects approximately 1% of adults and has been recognised as one of the most critical rheumatological conditions in the developed world [1], largely because of the associated joint damage, decline in functional status, and premature mortality [2]. The disease process leads to chronic and progressive inflammation involving multiple joints as well as other organ systems, and RA is associated with substantial disability and

Published online: 23 December 2011

economic losses [3], and even reduces life expectancy [4]. Treatment comprises medication to control inflammation and multidisciplinary interventions to reduce symptoms and maximise self-management [5].

RA leads to functional disability and possible changes in normal gait pattern, a common but clinically serious problem that substantially affects quality of life in RA patients [6]. Previous studies have demonstrated that RA may lead to a decreased walking speed [7], shortened stride length, and increased double-stance period [8], indicative of a limitation in lower limb function. Because of day-to-day variations in inflammatory activity and gait pattern in RA patients, self-monitoring and self-management becomes very important for controlling abnormal gait.

Recently, wireless tri-axial accelerometers have become widely used for gait analysis, because they are easy to use, are inexpensive, and do not require a laboratory environment. Several authors have performed gait assessment using such accelerometers in a clinical setting, including in patients with stroke, patients with Parkinson's disease, and older adults [9–11]. More recently, LeMoyne et al. [12] performed gait analysis experiments using a Smartphone, which demonstrated a capacity to accurately quantify gait parameters with a sufficient level of consistency. Similarly, our previous research showed that the smartphone gait analysis application has the capacity to quantify gait parameters with a degree of accuracy that is comparable to that of tri-axial accelerometers [Nishiguchi et al. unpublished observation].

The simplicity and portability of the smartphone application permits gait self-assessment by concerned individuals in a non-clinical setting. The aim of the present study was to examine the utility of the smartphone gait analysis application in patients with RA.

Methods

Participants

This was a cross-sectional study performed between April 2011 and May 2011 in the rheumatology outpatient clinics of Kyoto University Hospital. A total of 39 RA patients (mean age, 65.9 ± 10.0 years) participated. Patients with RA defined by the American College of Rheumatology 1987 criteria were included. The patients were assessed by an experienced rheumatologist. We excluded participants based on the following exclusion criteria: other musculoskeletal disorders, cognitive disorders, Parkinson's disease, stroke, or unable to walk unassisted over 15 m using current walking aids. Twenty older individuals (mean age, 69.1 ± 5.8 years) also took part in this experiment as control participants. We obtained written informed consent from each participant in accordance with the guidelines approved by the Kyoto University Graduate School of Medicine and the Declaration of Human Rights, Helsinki, 1975.

RA evaluation

For all patients, the following data were obtained: disease activity score (DAS) 28, modified health assessment questionnaire (mHAQ), and assessment of walking ability.

The DAS includes 4 parameters: number of joints tender to touch (out of 28 joints), number of swollen joints (out of 28 joints), C-reactive protein level, and patient-assessed disease activity using a 100-mm visual analogue scale. The DAS is generally accepted as a reliable, valid, and responsive measure of disease activity in patients with RA [13].

The mHAQ is a self-reported measure of physical function. The mHAQ is a widely used and validated tool to quantify functional disability in RA [14]. The mHAQ disability index assesses 20 daily living activities, including dressing and grooming, rising, eating, walking, hygiene, reach, grip, and community activities. The mHAQ is expressed on a scale ranging from 0 to 3 (where 0 = no functional disability and 3 = severe functional disability).

Assessment of walking ability was based on a subscale of the RA foot and ankle scale, which is expressed on a scale ranging from 0 to 20 (where 0 = unable to walk and 20 = no limitation) [15].

Gait analysis system

The smartphone (size: 63-mm width, 119-mm height, 13.1-mm depth; weight: 139 g; Xperia SO-01B; Android 2.1; Sony Ericsson Mobile Communications Japan, Inc.) used in this study includes an acceleration sensor, a recording device, and a computer program for processing the acceleration signals. Trunk linear accelerations were measured using the smartphone while the subject walked on the walkway. The smartphone was attached to the L3 spinous process using a semi-elastic belt (Fig. 1). Before measurements, the accelerometer of the smartphone was calibrated statically against gravity. The accelerometer of the smartphone sampled at 33 Hz. The recorded signals were analysed by the application developed in the android environment.

Gait analysis

The participants were instructed to walk on a 20-m walkway at their preferred speed. All participants wore their usual walking shoes, avoiding high heels and hard-soled shoes. The mid (10-m) walking time was measured using an electronic stopwatch.

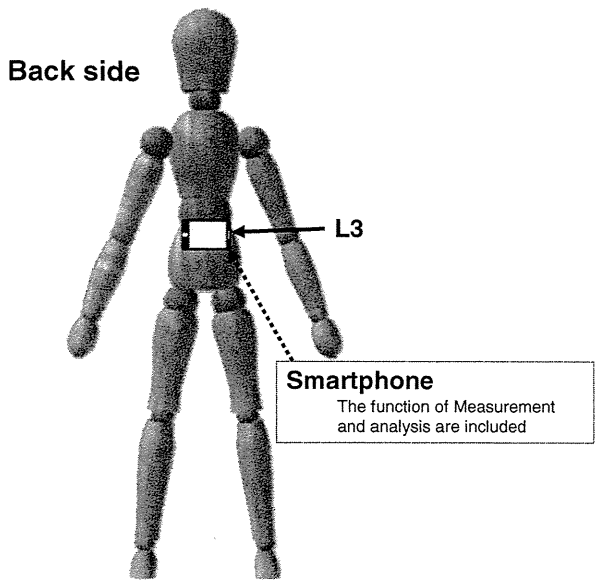

Fig. 1 Schematic representation of the use of the Smartphone, which was attached to the L3 spinous process, for gait assessment

Data processing

A period of steady state walking of 7.75 s was selected from the recording of each subject. This period contained about 256 acceleration measurements. We calculated the following gait parameters, according to previous studies: peak frequency (PF) [16], autocorrelation peak (AC) [16, 17], and coefficient of variance (CV) of the acceleration peak intervals [18, 19].

The PF value indicates the gait cycle, which is the time taken to take 1 step. The AC value indicates the degree of gait balance; the higher the AC value, the greater is the degree of balance. The CV value indicates the degree of gait variability, i.e., the variability in the elapsed time between the first contact of 2 consecutive footfalls. For calculating the gait parameters, we used the absolute values of the tri-axial acceleration data to decrease the influence of the measurement terminal posture. Let $a_{t_1:t_n} = a_{t_1}, a_{t_2}, \ldots, a_{t_n}$ denote the set of all acceleration absolute values acquired from time t_1 to t_n, for $t_1 \leq t_n$. Let a_t and n denote, respectively, the acceleration absolute value at time t and the number of all acceleration absolute values acquired from time t_1 to t_n.

PF f_p of acceleration data $a_{t_1:t_n}$ was detected with high accuracy based on the PF candidate f'_p, which was detected from the smoothed acceleration data in order to decrease the influence of the high-frequency measurement noise that accompanies PF detection. First, acceleration data $a_{t_1:t_n}$ was smoothed using a low-pass filter. Second, the PF candidate, f'_p, was detected where the power spectrum at frequency f'_p was the highest peak in the frequency space to which the smoothed acceleration data was converted by fast Fourier transformation. Finally, PF f_p was detected in the frequency space to which acceleration data $a_{t_1:t_n}$ was converted, where the power spectrum of PF f_p had the highest peak around PF candidate f'_p. The test–retest reliability using the inter-trial correlation coefficient (ICC 1.1) was 0.906 [Nishiguchi et al. unpublished observation].

AC R_p from the autocorrelation function was detected using PF f_p. This allowed us to detect AC R_p with a high degree of accuracy, based on the hypothesis that the gait cycle is related to the time lag when AC is detected [17]. The AC detection method was as follows: first, the autocorrelation function was calculated from acceleration data $a_{t_1:t_n}$. The autocorrelation function is represented by the sequence of the autocorrelation coefficients $R_{xx}(k)$ over increasing time lags k:

$$R_{xx}(k) = \frac{1}{n-k}\sum_{i=1}^{n-k} x_{t_i} x_{t_{i+k}} \quad (1)$$

Here, let x_t denote the normalised acceleration data, which are calculated by both the mean a_{MEAN} and standard deviation a_{SD} of acceleration data $a_{t_1:t_n}$; that is, $x(t) = a(t) - a_{\mathrm{MEAN}}/a_{\mathrm{SD}}$. Let n denote the number of acceleration data samples in our gait analysis. Finally, AC R_p was detected as the highest peak around the lag related to gait cycle T. The test–retest reliability using the ICC 1.1 was 0.752 [Nishiguchi et al. unpublished observation].

Coefficient of variance was calculated by using the group of positive peak time candidates detected in the smoothed acceleration data; this decreases the influence of the high-frequency measurement noise that accompanies positive peak detection. Here, the positive peak indicates the acceleration data with a positive convex shape on the acceleration waveform. First, acceleration data $a_{t_1:t_n}$ was smoothed using a low-pass filter. Second, each positive peak on the smoothed acceleration waveform was detected as a group of positive peak candidates. These measured times were extracted as a group of positive peak time candidates. Third, each positive peak of acceleration data $a_{t_1:t_n}$ was detected where each peak was the highest around each positive peak time candidate on the acceleration waveform. The time intervals between the neighbouring positive peaks were then calculated. Finally, CV is calculated from the mean t_{MEAN} and standard deviation t_{SD} of time intervals, as follows:

$$\frac{t_{\mathrm{SD}}}{t_{\mathrm{MEAN}}} \quad (2)$$

The test–retest reliability using the ICC 1.1 was 0.752 [Nishiguchi et al. unpublished observation].

Statistical analysis

Characteristics of RA and control groups were compared to examine the comparability of the 2 groups. Differences in the demographic variables and gait parameters between the 2 groups were analysed using the Student's t test or Chi-square test.

Criterion-related validity was determined by evaluating the correlation between gait parameters (PF, AC, and CV) and clinical parameters (DAS, mHAQ, walking ability, and walking speed) using Spearman's correlation coefficient in RA group. A multivariate analysis by means of multiple regression using a stepwise method was performed to investigate which of the gait parameters was independently associated with each clinical parameter in RA group. Data were entered and analysed using the SPSS program (Windows version 18.0, SPSS, Inc., Chicago, IL). A P value of <0.05 was considered statistically significant for all analyses.

Results

Characteristics of the participants are reported in Table 1. Typical acceleration waveforms are shown in Fig. 2.

Participants in the RA and control groups were comparable and well matched with regard to their baseline characteristics. There were no significant differences in age, body weight, height, or gender ($P > 0.05$). The RA group showed significantly lower scores for the walking speed, AC, and CV than the control group. There were no significant differences in PF (Table 1).

To determine the association between gait parameters and clinical parameters, we analysed Spearman's correlation coefficients (Table 2). PF was correlated with walking speed ($r = 280$, $P < 0.05$). AC was correlated with the DAS ($r = -0.283$, $P < 0.05$), mHAQ ($r = -0.368$, $P < 0.05$), and walking speed ($r = -0.704$, $P < 0.01$). CV was correlated with the DAS ($r = 0.334$, $P < 0.05$), walking ability ($r = -0.420$, $P < 0.01$), and walking speed ($r = 0.608$, $P < 0.01$). Walking speed was correlated with the mHAQ ($r = -0.442$, $P < 0.01$) and walking ability ($r = 0.413$, $P < 0.01$).

Stepwise regression analysis revealed that AC ($\beta = -0.435$, $P < 0.05$) was a significant and independent determinant of the DAS ($R^2 = 0.189$, $P < 0.05$). AC ($\beta = -0.368$, $P < 0.05$) was also a significant and independent determinant of the mHAQ ($R^2 = 0.135$, $P < 0.05$). CV ($\beta = -0.420$, $P < 0.05$) was a significant and independent determinant of the DAS ($R^2 = 0.232$, $P < 0.01$). PF ($\beta = -0.575$, $P < 0.01$) and AC ($\beta = -0.410$, $P < 0.01$) were significant and independent determinants of the DAS ($R^2 = 0.647$, $P < 0.01$) (Table 3).

Discussion

The results of the current study indicate that the RA group showed significantly lower scores for the gait parameters than the control group. Moreover, the clinical parameters were moderately associated with gait parameters recorded by a smartphone in patients with RA. We used the DAS, mHAQ, walking ability, and walking time as reference tools. The DAS index in RA patients reflects disease activity [13], and the mHAQ is often used for functional assessment in RA patients [14]. In this study, the DAS (disease activity) was associated with gait balance. The mHAQ (function) was also associated with gait balance. Further, walking ability was associated with gait variability, and walking speed was moderately associated with gait cycle and gait balance. Lelas et al. [20] found a mild correlation between kinematical measures of individual

Table 1 Comparison of demographic characteristics and gait parameters between the groups

	RA group		Control group		P value
	Mean	SD	Mean	SD	
Age (years)	65.9	10.0	69.1	5.8	0.189
Height (cm)	154.3	7.3	154.6	7.5	0.775
Weight (kg)	53.5	9.5	54.4	9.5	0.807
Gender female (n (%))	35 (89.7%)		15 (75.0%)		0.135
Disease duration (years)	11.9	9.4			
DAS (point)	3.2	1.4			
mHAQ (point)t	3.1	3.7			
Walking ability	15.9	4.9			
Walking speed (m/s)	1.03	0.26	1.30	0.54	<0.001
Peak frequency	2.13	0.25	2.03	0.08	0.073
Autocorrelation	0.735	0.122	0.796	0.081	0.037
Coefficient of variance (%)	15.1	10.0	9.2	3.8	0.011

DAS disease activity score, *mHAQ* modified health assessment questionnaire

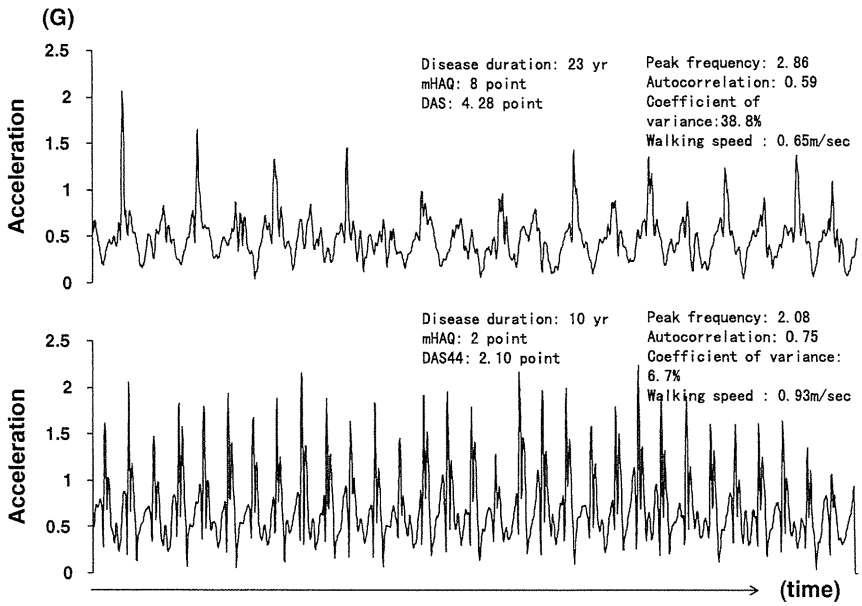

Fig. 2 The waveform of a patient with relatively severe rheumatoid arthritis (*top panel*) is irregular (peak frequency [PF] = 2.86, autocorrelation peak [AC] = 0.59, coefficient of variance [CV] = 38.8%, walking speed = 0.65 m/s). On the other hand, the waveform of a patient with relatively slight disease (*bottom panel*) is regular (PF = 2.08, AC = 0.75, CV = 6.7%, walking speed = 0.93 m/s). *DAS* disease activity score, *mHAQ* modified health assessment questionnaire

Table 2 Spearman's correlation coefficients for gait parameters and clinical parameters

	DAS	mHAQ	Walking ability	Walking speed
Peak frequency	−0.193	0.075	−0.247	0.280*
Autocorrelation	−0.283*	−0.368*	0.257*	−0.704**
Coefficient of variance	0.334*	0.155	−0.420**	0.608**
Walking speed	0.194	−0.442**	0.413**	

DAS disease activity score, *mHAQ* modified health assessment questionnaire

* $P < 0.05$; ** $P < 0.01$

joints and gait speed. Therefore, in systemic illnesses such as RA, it is possible that global waveform analysis is better than local waveform analysis for gait assessment. The results of the present study suggest that assessment of gait parameters using the smartphone is an acceptable method for evaluating gait in RA patients. Indeed, surprisingly, gait parameters measured by the smartphone were found to constitute an index of disease activity and physical function in patients with RA.

Self-management is important not only for patients with RA, but also for patients with other chronic disorders [21, 22]. Pain, disability, fatigue, and self-related general health are improved by systematic self-management educational programmes [21, 22]. Fatigue, especially, is difficult to control by medication and benefits from self-management [23]. The greatest benefit is observed if self-management programmes are maintained for over 8 years [24]. Online self-management systems have been constructed [25], and self-assessed walking ability, such as that described here, may be a useful addition to self-management systems.

The smartphone gait analysis application may be used as a clinical assessment tool and may also potentially be used as a standard method of self-assessment in RA patients, due to several benefits. First, it requires a shorter time for gait assessment in a non-clinical setting compared with traditional assessment tools. Second, it can be used to assess gait patterns easily in daily life. Third, medical practitioners and patients may be able to share information

Table 3 Multiple stepwise regression analysis for gait parameters and clinical parameters

Independent variables	DAS R^2 value = 0.189* Standard regression value	mHAQ R^2 value = 0.135* Standard regression value	Walking ability R^2 value = 0.232** Standard regression value	Walking speed R^2 value = 0.647** Standard regression value
Peak frequency				−0.575**
Autocorrelation	−0.435*	−0.368*		−0.410**
Coefficient of variance			−0.420**	

DAS disease activity score, *mHAQ* modified health assessment questionnaire

* $P < 0.05$; ** $P < 0.01$

regarding the patient's condition in real time by using the mobile phone function of the Smartphone. In consequence, patients may receive timely advice from their medical practitioner.

This study had some limitations. First, although the gait parameters correlated significantly with several clinical parameters, the correlation coefficients of some clinical parameters were not high. Gait parameters were only moderately correlated with global clinical measurements. Therefore, correlation coefficients may be high only for clinical parameters that reflect the walking pattern. Second, we did not consider disease stage, class, or history, drug use, or surgical history in our analyses. Further study is required to examine whether these factors have an influence on gait parameters. Third, the current study was of a cross-sectional design. A prospective cohort study and interventional study should be conducted in the future to further evaluate the relationship between gait parameters and clinical parameters.

In conclusion, this is the first study to examine the use of a smartphone device for gait pattern measurement. The results suggest that some gait parameters detected using the smartphone represent an acceptable assessment tool for gait in patients with RA.

Acknowledgments We would like to thank all the volunteers for participating in the study. We would also like to acknowledge the students of the Department of Human Health Sciences at Kyoto University for assisting in the data collection.

Conflict of interest Tatsuaki Ito, Shinyo Muto, and Tatsuya Ishihara are employees of NTT Cyber Solutions Laboratories. All other authors have no conflicts of interest to declare.

References

1. Silman AJ (1994) Epidemiology of rheumatoid arthritis. APMIS 102(10):721–728
2. Murphy D (1996) Lycra working splint for the rheumatoid arthritic hand with MCP ulnar deviation. Aust J Rural Health 4(4):217–220
3. Farr JN, Going SB, Lohman TG, Rankin L et al (2008) Physical activity levels in patients with early knee osteoarthritis measured by accelerometry. Arthritis Rheum 59(9):1229–1236
4. Myllykangas-Luosujärvi RA, Aho K, Isomäki HA (1995) Mortality in rheumatoid arthritis. Semin Arthritis Rheum 25(3):193–202
5. Luqmani R, Hennell S, Estrach C et al (2006) British Society for Rheumatology and British Health Professionals in Rheumatology guideline for the management of rheumatoid arthritis (the first two years). Rheumatology 45:1167–1169
6. Sakauchi M, Narushima K, Sone H et al (2001) Kinematic approach to gait analysis in patients with rheumatoid arthritis involving the knee joint. Arthritis Rheum 45(1):35–41
7. Laroche D, Pozzo T, Ornetti P et al (2006) Effects of loss of metatarsophalangeal joint mobility on gait in rheumatoid arthritis patients. Rheumatology 45(4):435–440
8. O'Connell PG, Lohmann Siegel K, Kepple TM (1998) Forefoot deformity, pain, and mobility in rheumatoid and nonarthritic subjects. J Rheumatol 25(9):1681–1686
9. Bautmans I, Jansen B, Van Keymolen B et al (2011) Reliability and clinical correlates of 3D-accelerometry based gait analysis outcomes according to age and fall-risk. Gait Posture 33(3):366–372
10. Mizuike C, Ohgi S, Morita S (2009) Analysis of stroke patient walking dynamics using a tri-axial accelerometer. Gait Posture 30(1):60–64
11. Lowry KA, Smiley-Oyen AL, Carrel AJ et al (2009) Walking stability using harmonic ratios in Parkinson's disease. Mov Disord 24(2):261–267
12. LeMoyne R, Mastroianni T, Cozza M et al (2010) Implementation of an iPhone as a wireless accelerometer for quantifying gait characteristics. In: Conference of the proceedings of IEEE Eng Med Biol Soc, pp 3847–3851
13. Prevoo ML, van't Hof MA, Kuper HH et al (1995) Modified disease activity scores that include twenty-eight-joint counts. Development and validation in a prospective longitudinal study of patients with rheumatoid arthritis. Arthritis Rheum 38(1):44–48
14. Bruce B, Fries JF (2003) The Stanford Health Assessment Questionnaire: a review of its history, issues, progress, and documentation. J Rheumatol 30(1):167–178
15. Niki H, Aoki H, Inokuchi S (2005) Development and reliability of a standard rating system for outcome measurement of foot and ankle disorders I: development of standard rating system. J Orthop Sci 10(5):457–465
16. Auvinet B, Berrut G, Touzard C (2002) Reference data for normal subjects obtained with anaccelerometric device. Gait Pos 16:124–134
17. Moe-Nilssen R, Helbostad JL (2004) Estimation of gait cycle characteristics by trunk accelerometry. J Biomech 37:121–126
18. Hausdorff JM, Rios DA, Edelberg HK (2001) Gait variability and fall risk in community-living older adults: a 1-year prospective study. Arch Phys Med Rehabil 82:1050–1056
19. Beauchet O, Allali G, Annweiler C et al (2009) Gait variability among healthy adults: low and high stride-to-stride variability are both a reflection of gait stability. J Gerontol 55:702–706
20. Lelas JL, Merriman GJ, Riley PO (2003) Predicting peak kinematic and kinetic parameters from gait speed. Gait Posture 17(2): 106–112
21. Barlow JH, Turner AP, Wright CC (2000) A randomized controlled study of the Arthritis Self-Management Programme in the UK. Health Educ Res 15(6):665–680
22. Foster G, Taylor SJ, Eldridge SE et al (2007) Self-management education programmes by lay leaders for people with chronic conditions. Cochrane Database Syst Rev 17(4):CD005108
23. Hewlett S, Ambler N, Almeida C et al (2011) Self-management of fatigue in rheumatoid arthritis: a randomised controlled trial of group cognitive-behavioural therapy. Ann Rheum Dis 70(6): 1060–1067
24. Barlow J, Turner A, Swaby L (2009) An 8-yr follow-up of arthritis self-management programme participants. Rheumatology 48(2):128–133
25. Smarr KL, Musser DR, Shigaki CL et al (2011) Online self-management in rheumatoid arthritis: a patient-centered model application. Telemed J E Health 17(2):104–110

The American Journal of Pathology, Vol. 178, No. 3, March 2011

DOI: 10.1016/j.ajpath.2010.12.012

Tumorigenesis and Neoplastic Progression

Murine Leukemia Retrovirus Integration Induces the Formation of Transcription Factor Complexes on Palindromic Sequences in the Signal Transducer and Activator of Transcription Factor 5a Gene During the Development of Pre–B Lymphomagenesis

Tatsuaki Tsuruyama,* Takuya Hiratsuka,† Guang Jin,‡ Yukiko Imai,* Haruya Takeuchi,* Yasuhiro Maruyama,§ Kazuya Kanaya,§ Munetaka Ozeki,* Tetsuya Takakuwa,‡§ Hironori Haga,¶ Keiji Tamaki,* and Takuro Nakamura‡

From the Departments of Forensic Medicine and Molecular Pathology and Human Health Science,§ Graduate School of Medicine, Kyoto University, Kyoto; the Laboratory of Pathology,† Noe-saiseikai Hospital, Osaka; the Laboratory of Carcinogenesis Cancer Institute,‡ Tokyo; and the Department of Diagnostic Pathology,¶ Kyoto University Hospital, Kyoto, Japan*

Murine leukemia retrovirus (MLV) vectors are highly effective tools for introducing a foreign gene into a target host genome. However, it remains unclear how integrated retroviral promoter activity is influenced by the upstream or downstream sequences and how the host cell phenotype is influenced by the integrated promoter activity. Herein, we analyzed a set of pre–B lymphoma clones in which the *MLV* genome was integrated into the signal transducer and activator of transcription factor 5a (*Stat5a*) gene. Among the clones, the lymphoma clones with a provirus integrating into the middle position of the palindromic target sequences showed significantly higher transcription of the *Stat5a* gene; and p300 and other transcriptional factors formed complexes, with binding to the proviral-host junctional DNA segment. By using a luciferase assay, the upstream and downstream sequences of the provirus contributed to the up-regulation of proviral promoter activity. In concomitance with the higher *Stat5a* transcription, the immunoglobulin gene recombination was arrested. Antiapoptotic activity was significantly higher, with an increase in Bcl-xL, one of the targets of STAT5A, when IL-7 was supplied. Thus, a minute difference between MLV integration sites can lead to large differences in the host phenotype through the formation of transcription factor complexes on the proviral-host junctional DNA segment, suggesting that caution is necessary in monitoring integration sites when working with MLV vectors. *(Am J Pathol 2011, 178:1374–1386; DOI: 10.1016/j.ajpath.2010.12.012)*

Retrovirus-based vectors have been used as an available tool for the introduction of a gene into the host genome in gene function analyses. Transgene transcription is predominantly controlled by the integrated retroviral promoter element in the long terminal repeat (LTR) in the vector sequence. However, because the retroviral promoter activity is affected by the integration site, the expression of a transgene is not necessarily adequate. The lack of control of retroviral integration limits its application in transgenic animal studies and gene therapy, which first and foremost must be safe for patients. Indeed, there is some risk that a murine leukemia retrovirus (MLV)–based vector could induce host malignant transformation by integration into an oncogene in the genome of a patient undergoing gene therapy.[1] Therefore, considerable attention has been given to the choice of appropriate vector integration sites for the induction of induced pluripotent stem cells from mouse embryonic or adult fibroblasts.[2] In fact, lack of control over

Supported by a Grant-in-Aid for Cancer Research from the Ministry of Education, Culture, Sports, Science and Technology of Japan and by the Ministry of Health, Labor and Welfare of Japan (grant 7013086 to T.N. and T.T.).

K.T. and T.N. contributed equally to this work.

Accepted for publication December 1, 2010.

None of the authors disclosed any relevant financial relationships.

Supplemental material for this article can be found at *http://ajp.amjpathol.org* or at doi:10.1016/j.ajpath.2010.12.012.

Address reprint requests to Tatsuaki Tsuruyama, M.D., Ph.D., Department of Forensic Medicine and Molecular Pathology, Graduate School of Medicine, Kyoto University, Yoshidakonoecho, Sakyo-ku, Kyoto 606-8501, Japan. E-mail: tsuruyam@fp.med-u.ac.jp or tsuruyam@kuhp.kyoto-u.ac.jp.

the integration site has limited the application of MLV vectors; it remains unclear to what extent the integration site influences retroviral promoter activity and host phenotype changes.

Furthermore, proviral promoter activity was compared under the expression of diverse—and not common—genes, which makes it impossible to render a consistent comparison. Because of these limitations associated with previous studies, the factors contributing to making proviral promoter activity exceedingly sensitive to minute nucleotide differences in the integration sites remain largely unstudied. The present investigation used comparative analysis of the activity of the MLV promoter integrated into an identical intron of the signal transducer and activator of transcription factor 5a (*Stat5a*) gene. We report that the activity is significantly influenced by the sequences flanking the retroviral integration sites and that the expression levels of the host gene can alter the host cell phenotype, as exemplified by hematopoietic cell differentiation and tumorigenesis induced by MLV integration.

In this article, we used a set of pro– to pre–B lymphoma clones containing the *MLV* genome integrated into variable sites within the second intron of the *Stat5a* gene, which is one of the common integration sites of MLV.[3,4] The encoded protein is a member of the STAT family and forms a dimer that translocates into the nucleus and exerts transcriptional activity by binding to the gamma interferon activation site element in the promoter of target antiapoptotic genes, such as *c-myc*, *pim-1*, *bclxL*, and cyclin D1,[5] that regulate proliferation and antiapoptosis in hematopoietic cells.[6,7] This signaling molecule in the IL-7 receptor pathway is limitedly operative during the precursor stage in the pro– to pre–B-cell lineage.[8] The STAT5A contributes to IL-7–induced B-cell precursor expansion.[9] Schwaller et al[10] have reported that *Stat5a* is essential for the myeloproliferative and lymphoproliferative diseases induced by Janus kinases. We supported their evidence by identifying the pro– or early pre–B-cell lymphomas using MLV integration into *Stat5a*.[4]

In the clones with MLV integration into *Stat5a*, we analyzed the correlation of the expression levels of the gene and MLV integration because varied STAT5A expression levels were expected to influence the degree of precursor expansion, probably affect Ig heavy chain (*IgH*) gene recombination in the host pre–B cells, and induce maturation arrest. To confirm the data on the MLV integration site and the expression levels of the target neighboring gene, we generated reporter gene assay vectors that consisted of the *MLV* genome either lacking or containing defective transcription factor–binding motifs within the retroviral LTR and the upstream and downstream sequences that originated from the *Stat5a* sequence. The downstream sequences were inserted upstream of luciferase as the reporter gene. Analysis of luciferase activity allowed us to investigate how different integration sites in the flanking sequence affect *MLV* promoter activity. Taken together, the data are consistent with the model presented herein for the control of retroviral promoter activity via interaction between the retroviral genome element and the host flanking sequence. The obtained data were used to construct a model demonstrating how a proviral genome in the target *Stat5a* sequence influences the proviral promoter activity and host cell phenotype.

Materials and Methods

Mice and Lymphoma Clones

All mice used in this study were handled in strict accordance with the guidelines for good animal practice, as defined by the relevant national and local animal welfare bodies; and all animal work was preapproved by the Kyoto University Ethics Committee for Animal Experiments. The SL/Kh mice were obtained from the RIKEN Bioresource Center, Tokyo, Japan. This strain possesses a pathogenetic endogenous ecotropic murine virus (*Emv11*) that was mapped on chromosome 7,[11] which is shared with the AKR/J mouse strain.[12] In addition, more than five copies of the endogenous murine leukemia retroviral genome, in addition to *Emv11*, are observed (Figure 1B, left). The identified endogenous MLV genomes are shown in Supplemental Table S1 (at *http://ajp.amjpathol.org*).

In the SL/Kh strain, the pro– to pre–B cells in the bone marrow (BM) acquire more than one copy of the proviral genome; and more than 90% of these mice develop BP-1$^+$ sIgM$^-$ pro– or pre–B lymphomas spontaneously by the age of 6 months.[4,11] Lymphoma cells of the swelling lymph node, 2.0×10^8, were obtained from a lymph node of a 6-week-old SL/Kh mouse and incubated in methylcellulose-based medium (Methocult) containing IL-7 for pro– to pre–B cells (Stemcell Technology, Vancouver, British Columbia, Canada) or in RPMI 1640 medium (Invitrogen, Carlsbad, CA) with 20-ng/ml IL-7, IL-3, IL-4, or stem cell factor (Peprotec, London, England).[4]

Southern Hybridization to Detect MLV Insertional Recombination in Stat5a

High-molecular-weight DNA samples were extracted from lymphoma and normal kidney tissues, and 2.5-mg aliquots of the DNA were digested with the NcoI restriction enzyme (New England Biolabs, Beverly, MA) for 16 hours and transferred to an N$^+$ nylon membrane (Hybond; GE Health Care, Buckinghamshire, England) after electrophoresis. The probe used was previously described.[4]

Inverse PCR Method for the Detection of the MLV Integration Site

The inverse PCR method was previously described.[4] The primers for inverse PCR were located within the *MLV* (EmvII) genomes. Their sequences were as follows: 5B4, 5′-GAGGGCTTGGACCTCTCGTCTCCTAAAAAACCACG-3′; and 5F1, 5′-GTCTCTCCCAAACTCTCCCCCTCTCCAACC-3′ (first set). In addition, these sequences were used: 5F2, 5′-CCTCCTCTGACGGAGATGGCGACAGAGAAGAGG-3′; and 5B1, 5′-GAGGGCTTGGACCTCTCGTCTCCTAAAA-GAACCACG-3′ (second step of the cycles for nested PCR). The amplicons were then subcloned into a vector (pCR 2.1-TOPO; Invitrogen), and sequence analysis reactions were performed.

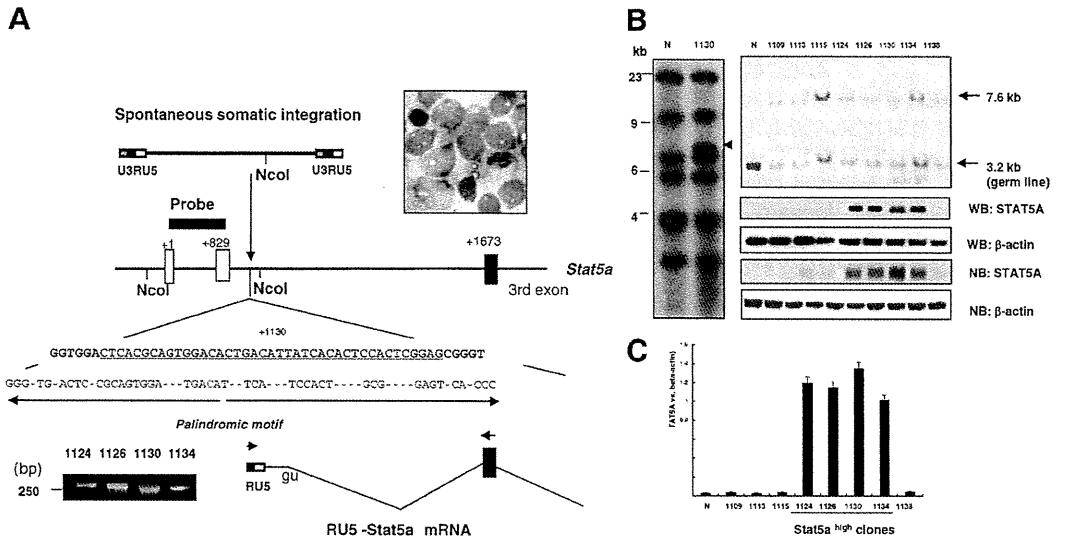

Figure 1. Genome integration of MLV provirus into *Stat5a*. **A:** Clones with MLV integration into the second intron of *Stat5a* (GENEBANK, AF049104). The two open boxes and the closed box in the *Stat5a* structure represent the untranslational exons and the third translational exon, respectively. The numbers represent the nucleotide number from the start of the gene. The detailed sequence of the integration site is shown. The underlining represents the flanking sequence used in the **i** through **vi** vector constructs in Figure 2A. The red letter in the sequence represents the position of integration site 1130 within the intron. Palindromic sequence motifs are shown at the bottom. NcoI sites are shown. The upper **inset** shows blastic lymphoma tissue from SL/Kh mice (Giemsa staining, original magnification ×600). Probe indicates the position of the probe used in the Southern hybridization assay.[4] The MLV-*Stat5a* chimera mRNA is shown below. The represented *gu* motif is the splicing signal sequence at the 1158 nucleotide. The bottom shows the result of the RT-PCR assay for chimera cDNA, including MLV RU5 (69 bp), the second intron (24 to 34 bp), and the third exon (158 bp) of *Stat5a*. Lane numbers represent the integration sites. **Arrows** represent the PCR primer positions. **B:** Southern blot of an NcoI-digested DNA fragment displaying the insertional recombination. **Left:** Six copies of an endogenous retroviral genome (N, 1130) and a newly acquired proviral genome (1130, **arrowhead**). **Right:** *Stat5a*-derived fragments are visualized. The upper **arrow** highlights the NcoI-digested fragment obtained after *Emv11* integration. Lane numbers represent the integration site. N indicates control BM pre–B cells of SL/Kh mice 3 weeks after birth; WB:STAT5A, Western blot of the lymphoma extract with an antibody for STAT5A. Fragments of 7.6 kb represent the NcoI-digested fragment obtained after MLV clonal integration. (β-Actin was the control blot.) NB:STAT5A is the Northern blot of lymphoma mRNA. (β-Actin was the control blot.) **C:** Relative intensity of STAT5A versus β-actin (control). The horizontal axis represents the nucleotide number from the start of the first exon of the *Stat5a* gene.

PCR for the Detection of Recombination in IgH and Ig Light Chain

The monoclonality was confirmed by PCR analysis after IgH diverse segment (D_H)–IgH J segment (J_H) recombination using primers designed to amplify four possible junctions between the D-Q52 and J_H regions. The primers were as follows: 5′-CACAGAGAATTCTCCATAGTTGATAGCTCAG-3′ (D_HQ52-1 [sense]) and 5′-AGGCTCTGAGATCCCTAGACAG-3′ (J_H4-1 [antisense]). The PCR conditions were as follows: denaturation for 1 minute at 95°C, annealing for 1 minute at 60°C, and extension for 2.5 minutes at 72°C (28 cycles). After D_H-Q52–J_H recombination, the monoclonal lymphoma cells were selected from the other cells and used for the following assays. For the analysis of V-J rearrangement, the degenerate V primer and another primer were used to amplify Vκ to J1-5κ rearrangement, as previously described.[13]

Flow Cytometry

A suspension of single cells was prepared from lymphoma tissue. The cells were adjusted to 10^6 cells/ml; the total lymphoma cell yield was in the range of 0.8×10^7 to 1.2×10^7 cells. A single-cell suspension was prepared from both SL/Kh and BALB/c mouse femur BM plugs, and their densities were adjusted to 10^6 cells/ml. The following antibodies were purchased commercially (BD Pharmingen, San Diego, CA): fluorescein isothiocyanate–labeled anti-BP1 (clone 6C3) and phosphatidylethanolamine-labeled anti-B220 (clone RA3-6B2). The collected cells were incubated with normal rat serum for 15 minutes and stained with 1:10,000 diluted monoclonal antibodies for 15 minutes. After washing, the cells were analyzed using a scanner (FACScan; Becton Dickinson, Mountain View, CA). The $BP1^+B220^+$ BM cells were purified from double-stained BM cells by cell sorting using a commercially available system (FACS Vantage; Becton Dickinson). The average yields from the BM cells of 4-week-old BALB/c and SL/Kh mice were 0.50% and 2.8%, respectively. Genomic DNA was extracted from the purified cells using a kit (QIAamp DNA Blood Mini Kit; QIAGEN GmbH, Hilden, Germany). Apoptotic lymphoma cells, 0.8×10^7 to 1.2×10^7, were stained using 5 ml of phosphatidylethanolamine-conjugated antibody (annexin V) at room temperature in the dark for 15 minutes. A 400-ml binding buffer was added for flow cytometry analysis.

Northern Blotting and RT-PCR Assay

The methods were previously described.[4] The RT-PCR was performed using extracted RNA with a one-step RT kit (Invitrogen). The primers used were as follows: actin, 5′-CCTAAGGCCAACCGTGAAAAG-3′ and 5′-TCTTCATGGTGCTAGGAGCCA-3′; terminal deoxytransferase, 5′-GAAGATGGGAACAACTCGAAGAG-3′ and 5′-CAGGTGCTGGAACATTCTGGGAG-3′; *Vpreb*, 5′-CGTCTGTCCTGCTCATGCT-3′ and 5′-ACGGCACAGTAATACACAGCC-3′;

CD79a, 5′-ATCACATGGTGGTTCAGCC-3′ and 5′-TCTCCAATGTGGAGGTTGC-3′; and *CD19*, 5′-TGTCTCTTCTGAGAAGCTGGC-3′ and 5′-AACCAGAAGTGGACCTGTGG-3′. The RT-PCR primers for the Ig κ light chain were as follows: 5′-GGCTGCAGSTCCAGTGGCAGTGGRTCWGGRAC-3′ and 5′-CATTCCTGTTGAAGCTCTTGACAATGGGTG-3′. The RT-PCR primers for the Ig λ light chain were as follows: forward, 5′-GCCTTTCTACACTGCAGTGGGTATGCAACAAT-3′; and reverse, 5′-AGCCACTYACCTAGGACAGTSASYTTGGTTCC-3′. For real-time PCR assays for the detection of proviral RNA in the lymphomas, total RNA was reverse transcribed using a kit (Omniscript RT kit; Qiagen). For relative quantification by RT-PCR, 20 ng of each cDNA was analyzed using a kit (FastStart DNA Master SYBR Green I; Roche Diagnostics, Mannheim, Germany) with software version 3.5. For each primer pair, a standard curve was developed. To detect *Emv11-Stat5a* chimera RNA, the following primer set was used: MLV U5–*Stat5a* exon3-1F, 5′-GAATCGTGGTCTCGCTGATC-3′; and MLV U5–*Stat5a* exon 3-1R, 5′-CCTGGAGCTGTGTGGCATAG-3′.

Antibodies for Western Blotting of STAT5A

Cell lysate was precleared using protein G–Sepharose (Sigma-Aldrich, St Louis, MO) at 4°C with 1 hour of agitation. The cleared lysate, 400 μL, was incubated with minimal essential medium 59, 50 μL, at 4°C overnight; then, protein G–Sepharose, 50 μL, was added and incubated for an additional hour. After centrifugation, immunocomplexes were washed three times with a radioimmunoprecipitation assay buffer (25 mmol/L Tris-HCl, pH 8.0; 150 mmol/L NaCl; and 1% NP40, a protease inhibitor mixture [Complete Mini EDTA-free; Roche Diagnostics]), resuspended in the sample buffer, and boiled for 5 minutes. The released proteins were examined by Western blotting. Antityrosine phosphorylated STAT5A was purchased from New England BioLabs (Ipswich, MA) and Santa Cruz Biotechnology (Santa Cruz, CA) (sc-11761). Purified anti-STAT5A and anti-STAT5B were obtained from ZYMED (San Francisco, CA). Antibodies toward β-actin (C4), p300 (sc-81349), GATA1 (sc-266), GATA2 (sc-267), Runx1 (sc-28679), Bcl-xL (sc-7122), CREB (sc-20), and CRE-BP1 (sc-8398) were also purchased from Santa Cruz Biotechnology (sc-47778). Streptavidin-peroxidase conjugate was acquired from DAKO (Gostrup, Denmark). The blot was measured using a chemiluminator (Aishin, Nagoya, Japan).

Vector Construction and Dual Luciferase Assay

For a reporter gene assay, Ba/F3 cells were obtained from RIKEN cell bank (Tsukuba, Japan). After a 12-hour recovery period in the 10-ng/ml IL-3–containing medium, the cells were incubated in an RPMI 1640 medium supplemented with 0.5% bovine serum albumin for 12 hours or stimulated with the cytokine for the last 6 hours. The Ba/F3 cells, 6.0×10^7, were transiently transfected by electroporation with 5 μg of a luciferase reporter plasmid. Electroporation was performed according to a previously reported protocol.[14] In each experiment, samples were analyzed in triplicate; and each experiment was repeated five times. On the other hand, lymphoma cells with the provirus integrating into *Stat5a* were maintained in an RPMI 1640 medium supplemented with 20% fetal calf serum, mercaptoethanol, and 50-mg/ml penicillin-streptomycin. Reporter gene analysis was performed 48 hours after transfection (Tecan, Durham, NC).

Cell lysate was then subjected to an assay (Dual-Luciferase Reporter Assay System; Promega, Madison, WI); a pGL3-basic vector lacking SV40 promoter (Promega) was used as the backbone for *Emv11*-derived provirus-firefly luciferase vectors (o, i, ii, iii, iv, v, vi, and vii) in the current study. The HindIII site (+53) in the multicloning site of the pGL3-basic vector was used to construct the firefly luciferase vector, including the *Emv11* proviral genome that was inserted into the identical orientation of the firefly luciferase and the flanking *Stat5a* sequence shown in the o through vii constructs for the assay. The flanking *Stat5a* sequence originated from the second intron. As a control for luciferase measurements in transfections, pRL-TK (HSV-tymidine tyrosine kinase) renilla luciferase (Promega) was cotransfected with a firefly luciferase vector. Firefly luciferase activity was normalized to renilla luciferase activity.

Preparation of MLV Integrase and Anti-Integrase

Full-length murine retroviral integrase cDNA (GENEBANK, J01998) was obtained from an SL/Kh mouse and subcloned into multiple cloning sites (EcoRI and XhoI) of the transfer vector (pSYNGCH; Katakura Industries, Saitama, Japan). The procedures for the construction of the recombinant virus and viral infection of silkworm *Bombyx mori* larvae have been reported.[15] To construct the recombinant baculovirus, Abv baculovirus DNA, a linearized AcNPV-BmNPV hybrid-type baculovirus DNA (Katakura, Maebashi, Japan), 0.5 mg, and psYNGCH-Th integrase, 1 mg, were used to cotransfect a monolayer of BmN cells, 2×10^6 cells/ml, in the presence of liposomes (Insectin; Invitrogen). These cotransfected BmN cells were maintained at 27°C in a culture for 5 days. Silkworm pupae were infected with the supernatants and harvested after 6 days. The pupae were homogenated by suspension in 30 ml of ice-cold homogenizing buffer A (20 mmol/L Tris-HCl, 150 mmol/L NaCl, 1 mmol/L EDTA, 1 mmol/L EGTA, 1 mmol/L dithiothreitol [DTT], and 0.05% phenylthiourea, pH 8.0) containing a protease inhibitor mixture (1 mmol/L phenylmethanesulfonyl fluoride and 10 mmol/L benzamidine) and disrupted at 3000 rpm for 5 minutes. The homogenate was centrifuged at 38,000 rpm for 1 hour at 4°C. After removal of the supernatant, the pellet was suspended in 30 ml of homogenizing buffer B (20 mmol/L Tris-HCl, 150 mmol/L NaCl, 1 mmol/L EDTA, 1 mmol/L EGTA, 1 mmol/L DTT, and 0.05% phenylthiourea, pH 8.0) containing the protease inhibitor mixture and thoroughly mixed in a homogenizer (Dounce Teflon) on ice at 1000 rpm for 10 strokes. The EDTA and DTT were added to the pellet at a final concentration of 10 mmol/L, followed by solubilization with a sulfobetaine detergent (Zwittergent 3-12; Calbiochem, San Diego). The

final concentration of the detergent was 2% w/v. The sample was stirred gently for 1 hour at 4°C and then centrifuged (Hitachi RP50-2 rotor) at 38,000 rpm for 1 hour at 4°C. The supernatant was collected, and the integrase was purified by column chromatography using the His-tag expressed on the integrase. Because integrase tended to aggregate, we immediately used it in assays after the purification. The obtained integrase was immediately injected into rabbits for immunization for the production of polyclonal anti-integrase. The molecular weight of the recombinant integrase was confirmed by Western blot analysis using the prepared antibody.

RNAi of Stat5a and Stat5b

The *Stat5a* RNAi (sc-37009; Santa Cruz Biotechnology) and the homologue *Stat5b* RNAi or control small-interfering RNA (siRNA) (sc-37007) were used according to the manufacturer's protocol (Santa Cruz Biotechnology). In a six-well tissue culture plate, 8.0×10^5 cells were seeded per well in a 2-ml antibiotic-free normal growth medium supplemented with fetal bovine serum. The lymphoma cells were incubated for 18 to 24 hours at 37°C in a CO_2 incubator. The siRNA duplex solution (solution A) was added directly to the diluted transfection reagent (solution B) using a pipette. The lymphoma cells were washed once with 2 ml of an siRNA transfection medium (sc-36868), and the medium was aspirated. We proceeded immediately to the next step. For each transfection, 0.8 ml of an siRNA transfection medium was added to each tube containing the siRNA transfection reagent mixture (solution A plus solution B). After gentle mixing, the mixture was overlaid onto the washed lymphoma cells, and the cells were incubated for 5 to 7 hours at 37°C in a CO_2 incubator. One milliliter of the normal growth medium containing twice the normal serum and antibiotic concentration (×2 normal growth medium) was added without removing the transfection mixture. Because of low viability, we removed the transfection mixture and replaced it with a ×1 normal growth medium. Next, the cells were incubated for an additional 96 hours. The medium was aspirated and replaced with fresh normal growth medium, and the protein was extracted and assayed by Western blotting using anti-STAT5A (ZYMED).

Preparation of Nuclear Extracts and Electromobility Shift Assay

The methods were previously described.[4] The probes were double-stranded oligonucleotides corresponding to the Stat-binding motif on the *bclxL* gene promoter (5′-GACTTTCCGAGGAAGGCATTTCGGAGAAGAC-3′). For a competition study, the extracts were incubated with 150 mol/L excess of the unlabeled probe.

Chromatin Immunoprecipitation Assay

The chromatin immunoprecipitation (ChIP) assay was performed as previously described.[14,16] The SL/Kh pre–B lymphoma clones were fixed with 1.0% formaldehyde at 4°C for 1 hour. Soluble chromatin was immunoprecipitated with 4 mg of primary antibodies overnight. The immune complex was eluted by incubation with a buffer containing 10 mmol/L DTT at 37°C for 30 minutes, diluted 50-fold, and reimmunoprecipitated with the second antibody. The same sets of fivefold serial dilutions of input DNA for determining the appropriate DNA concentration in the absence of nonspecific amplification and 2.5% to 5% purified ChIP DNA were subjected to PCR for 28 to 30 cycles. Control primers were used for determining the appropriate dilution.[14] After confirming that the nonspecific amplification was not observed by dilution, the immunoprecipitated DNA was amplified using the following primers: exon3 of *Stat5a*, 5′-CACGGCTGGCTCTCGATCCAC-3′; and, for the repeat region in 3′-LTR of *Emv11*, 5′-CAATAAAGCCTTTTGCTGTTGC-3′. To amplify the provirus 5′-LTR-*Stat5a* junctional DNA, the following primers were used: exon2 of *Stat5a*, 5′-CAAGAGCCGTCAGGAGCCGTC-3′; and, for the repeat region in 5′-LTR of *Emv11*, 5′-CAGATATCCTGTTTGGCCCTAG-3′. To amplify the provirus 5′-LTR (U3RU5), the following primers were used: 5′-TGAAAGACCCCTTCATAAGGCTTA (U3)-3′ and 5′-GGCTCCGTGGAAGAACTGAC-3′. To amplify the provirus 3′-LTR (U3RU5), the following primers were used: 5′-AGACAGGATTTCGGTAGTGCAGG (P15E)-3′ and 5′-ACAGCAAAGGCTTTATTGG-3′.

Statistical Analysis

Results are expressed as mean ± SD unless otherwise stated. All statistical analyses were performed using computer software (StatView; Abacus Concepts, Berkeley, CA). An unpaired *t*-test was used.

Results

MLV Integration Sites in the Stat5a *Gene*

In the current study, we analyzed a set of lymphoma clones with the *Emv11*-derived provirus integrated into the second intron of *Stat5a* (Figure 1A).[4] Integration sites were frequently found within a 46-bp palindromic sequence, including the most frequent site (ie, 1130). Southern hybridization using the MLV env probe or the *Stat5a* DNA probe demonstrated a newly acquired *MLV* genome integrating into *Stat5a* (Figure 1B, left and upper right).

There were significant differences in the expression level of STAT5A between the clones, whereas there were only minute differences in the integration sites; proviral genomes were identical. In particular, the expression of STAT5A was significantly higher in the lymphoma cells, with integration into sites between 1124 and 1134; in contrast, expression was not obvious in lymphoma cells with integration into other sites (Figure 1B, upper right, and Figure 1C). Thus, a minute difference between MLV integration sites led to large differences in the expression level of the target *Stat5a*. For the following analysis, we divided the clones into two groups on the basis of the expression level of STAT5A. Because constitutively and highly expressed STAT5A was observed in the clones with MLV integration into the 1124 to

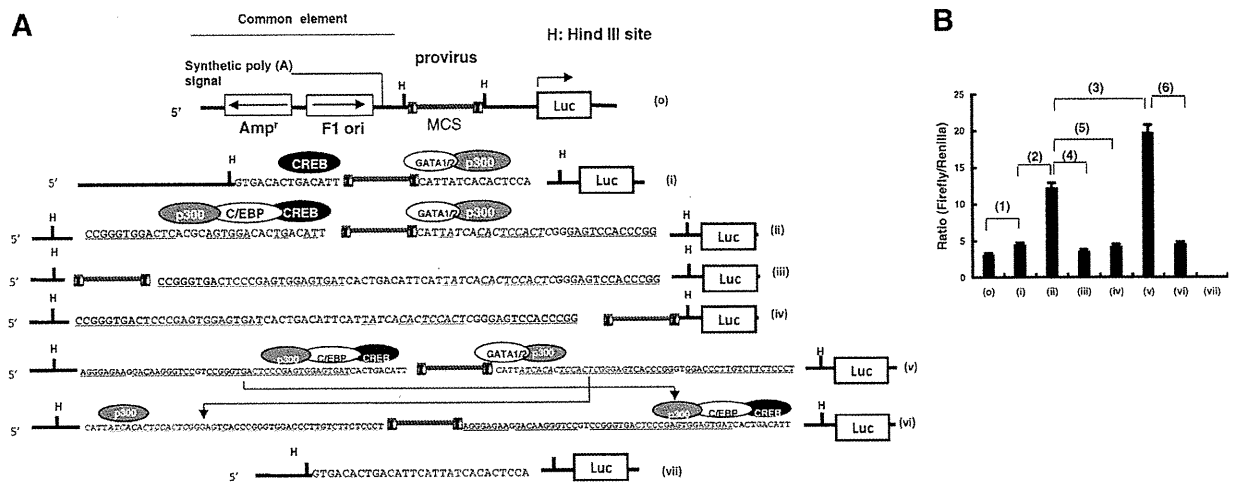

Figure 2. Luciferase assay using the Stat5a-derived sequence and *MLV* provirus genome. **A:** Sequences of the luciferase assay vectors. **o**, The pGL3-*Emv11* vector did not have the MLV flanking sequence. The pGL3 structure is shown. Luc represents Firefly luciferase in the pGL3 basic vector. The sequences of **i** through **vi** pGL3 vectors included the sequences flanking the proviral genome from the *Stat5a* sequence. MCS represents the location of the HindIII site (H) in the multiple-cloning site. **o**, **i**, **ii**, **iii**, **iv**, **v**, and **vi** in the schemes represent the ligated position of the provirus. The underlined letters indicate the palindromic motifs in the flanking sequences. The colored sequence is identical to the *Stat5a* sequence displayed in Figure 1A. The oligonucleotides CATT flanking the provirus were duplicated at the 5′ and 3′ ends of the provirus because such duplication in the integration site is commonly observed in *Emv11* integration sites. Red CATTATC at the 3′ end of the provirus is the GATA family binding sequence. Italicized *ATCACACTCCACTC* at the 3′ side flanking sequence is the p300 binding sequence. In the **iii**, **iv**, and **v** vectors, the proviral genome was flanked by identical sequences at different sites. **Arrows** in **v** and **vi** indicate the reverse of the flanking sequence in **v** for making the **vi** construct. Vector **vii** was the negative control vector, including the *Stat5a* sequence alone. **B:** Luciferase activity (ratio of Firefly to Renilla luciferase signal) in Ba/F3 cells containing vectors. Individual assays were independently performed five times. Individual columns represent the data obtained using the five vectors indicated. **o** through **v** represent the integration sites of the provirus (n = 5; 1, **o** versus **i**, P = 0.031; 2, **i** versus **ii**, P = 0.024; 3, **ii** versus **v**, P = 0.011; 4, **ii** versus **iii**, $P < 0.001$; 5, **ii** versus **iv**, $P < 0.001$; and 6, **v** versus **vi**, $P < 0.001$). Table 1 contains additional information. Luciferase activity values were evaluated using the Student's t-test.

1134 segment, they were named Stat5a^{high} clones. On the other hand, clones with integration into other sites were named Stat5a^{low} clones.

Furthermore, to evaluate how STAT5A expression was promoted by the integrated *MLV* genome, we attempted to analyze MLV-LTR-*Stat5a* chimera RNA. We found that the downstream *Stat5a* intron was serially transcribed after the RU5 element in the 5′-LTR of the provirus (Figure 1A). Therefore, the U3 segment of the 5′-LTR probably functioned as a promoter that up-regulated the expression of STAT5A.

Upstream and Downstream Sequences of the Provirus Influenced Reporter Gene Expression

The integration hot spots are within a 46-bp palindromic region containing transcription factor–binding sites. To examine whether the flanking sequence of the integration site might influence proviral promoter activity, luciferase assays were performed using seven pGL3-MLV-luciferase vectors consisting of a provirus or the downstream sequence, including CREB-, GATA-, and p300-binding motifs in *Stat5a* (Figure 2A). The Ba/F3 cells were selected for the assay because of their relative phenotypic similarity to the studied lymphoma cells, and luciferase reporter plasmids were transfected. Firefly luciferase activity was significantly up-regulated when the vector consisting of intact *Emv11*-derived proviral genome was flanked by the *Stat5a* sequence. In particular, activity was stronger when the *Emv11* proviral genome was flanked by a longer *Stat5a* sequence: 1, P = 0.031, o versus i; 2, P = 0. 024, i versus ii; and 3, P = 0.011, ii versus v (Figure 2B). Of particular interest are vectors ii, iii, and iv, in which a proviral genome was integrated into different positions in the palindromic sequence, indicating that the symmetric location of the provirus in vector ii may be a critical factor for the higher activity of the promoter (4, $P <$ 0.001, ii versus iii; and 5, $P < 0.001$, ii versus iv) (Table 1 and Figure 2B). In addition, the use of vector vi, which has the reverse flanking sequence of v, resulted in significant down-regulation of luciferase (6, $P < 0.001$, v versus vi) (Figure 2B), indicating that the flanking GATA- and p300-binding motifs also influence promoter activity.

Table 1. Results of the Dual Luciferase Assay Using Modified Emv11 Genomes

Vector	*Emv11*	*Emv11-5′Runx1-*	*Emv11-3′Runx1-*	*Emv11-5′LTR*	*Emv11-3′LTR*
i	0.008*	0.019*	0.021*	0.036*	0.214
ii	0.007*	0.028*	0.039*	0.018*	0.432
iii	0.071	0.267	0.398	0.291	0.291
iv	0.067	0.358	0.556	0.791	0.405
v	0.009*	0.032*	0.013*	0.012*	0.561

Data are given as P values for vector o versus five other vectors.
*Significant difference between vectors.

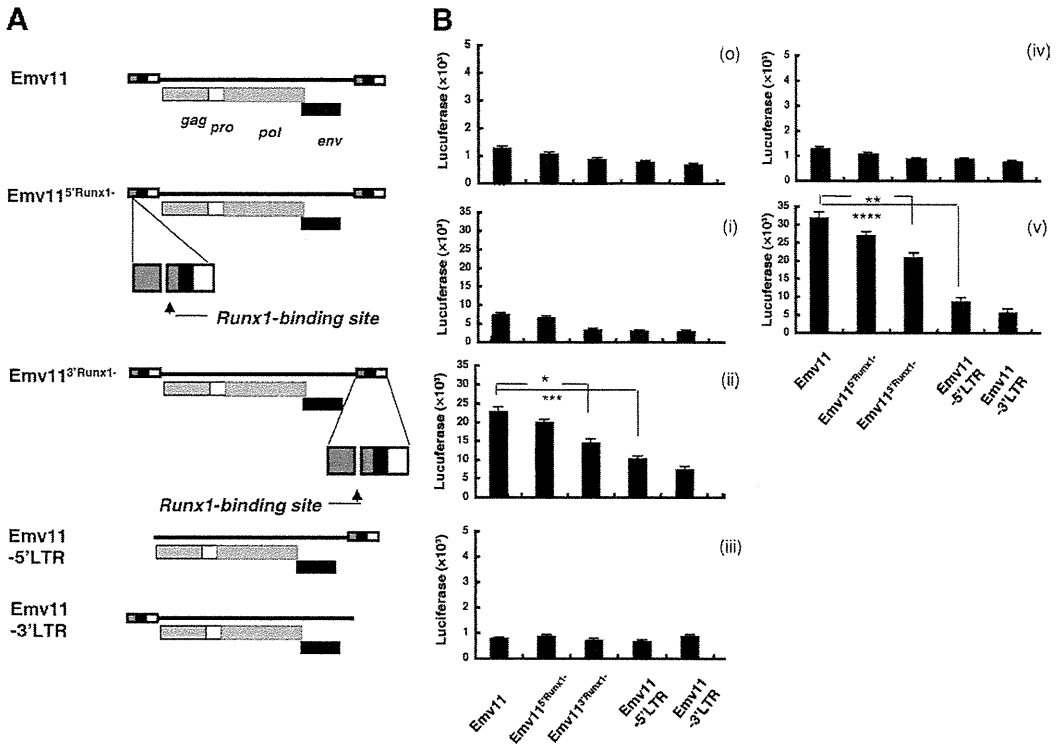

Figure 3. Luciferase assay using modified *Emv11* genomes. **A:** Structure of *Emv11* constructs in the luciferase assay vectors. Native *Emv11* is displayed at the top. Gag (group specific antigen), pro (protease), pol (polyprotein), and env (envelop protein) denote common retroviral genome elements. *Emv11*$^{5'Runx1-}$ and *Emv11*$^{3'Runx1-}$ represent *Emv11* lacking the *Runx1*-binding motif in 5′-LTR and 3′-LTR, respectively. *Emv11-5′-LTR* and *Emv11-3′-LTR* represent *Emv11* lacking 5′-LTR and *Emv11* lacking 3′-LTR, respectively. **B:** Luciferase assays. Luciferase activity (ratio of Firefly to Renilla luciferase signal) in Ba/F3 cells containing vectors. Individual assays were independently performed five times. Individual columns represent the data obtained using the five vectors indicated. **i** through **v** represent the vectors used. Table 2 contains additional information. For **ii**, $^{*}P = 0.032$; $^{***}P = 0.028$; **v**, $^{**}P = 0.041$; $^{****}P = 0.012$. Luciferase activity values were evaluated using the Student's *t*-test.

Activity of the Proviral Promoter Element

Next, we prepared five Firefly luciferase pGL3 vectors (o-v) at the HindIII site in the multicloning site into which defective proviral cDNA was inserted. These proviral DNAs in the vectors had defects in 3′-LTR (*Emv11*-3′-LTR), 5′-LTR (*Emv11*-5′-LTR), the Runx1-binding motif in 5′LTR (*Emv*$^{5'Runx1-}$), or the Runx1-binding motif in 3′-LTR (*Emv*$^{3'Runx1-}$) (Figure 3A). The vectors o through v carrying individual proviral cDNA were transfected into Ba/F3 pro–B cells.

The results showed that Firefly luciferase is significantly up-regulated even when the vector includes defective proviral genomes that are symmetrically flanked by palindromic motifs, as observed using intact *Emv11* vectors (Figure 3B and Table 1; $P < 0.05$ for i, ii, and v versus o). There were significant increases in luciferase activity when using *Emv11* inserted into ii and v instead of *Emv*$^{3'Runx1-}$ inserted into ii and v [Figure 3B ($^{*}P = 0.032$ and $^{**}P = 0.041$) and Table 2 ($n = 5$, ii and v)]. In addition, there were significant increases when using *Emv11* inserted into ii and v instead of *Emv11-5′LTR* (Figure 3B [$^{***}P = 0.028$ and $^{****}P = 0.012$] and Table 2 [$n = 5$, ii and v]). These data suggested that the Runx1-binding motif in 3′-LTR contributed to the up-regulation of downstream Firefly luciferase.

GATA2-Binding Motif in the Flanking Sequence

We analyzed the sequence motifs of the flanking sequences in host clone genomes. The GATA2-binding motif 5′-CAT-

Table 2. Results of the Dual Luciferase Assay

	Emv11 versus			
Vector	*Emv11-5′Runx1-*	*Emv11-3′Runx1-*	*Emv11-5′LTR*	*Emv11-3′LTR*
i	0.075	0.064	0.056	0.019*
ii	0.063	0.046*	0.028*	0.012*
iii	0.051	0.452	0.056	0.215
iv	0.085	0.673	0.081	0.366
v	0.062	0.037*	0.012*	0.006*

Data are given as *P* values for *Emv11*-carrying vectors versus individual defective *Emv11*-carrying vectors.
*Significant difference between vectors.